Identification of mechanical properties of laminates

Rolands Rikards

Institute of Materials and Structures, Riga Technical University, Latvia

Abstract. Identification

1 Formulation of Identification Problem

Discussing the role of experimental mechanics in an increasing computational capabilities Knauss (2000) emphasized that now it is possible to extract physical information from more involved experiments that previously. In this direction during the last decade investigations for developing a new technique for material identification, the so-called mixed numerical-experimental technique, have started. Employing this technique a laminate stiffness properties have been investigated by Pedersen; Soares et al.; Grediac and Vautrin; Sol et al.; Frederiksen (1989; 1993; 1993; 1993; 1997a).

The determination of stiffness parameters for complex materials such as fiber reinforced composites is much more complicated than for isotropic materials since composites are anisotropic and non-homogeneous. Conventional methods for determining stiffness parameters of the composite materials are based on direct measurements of strain fields, i.e., using information at a point of solid only. Boundary effects, sample size dependencies and difficulties in obtaining homogeneous stress and strain fields are some of the most serious problems. As a result of this, indirect methods using mainly a field information have recently received increasing attention. One such indirect method is based on measurements of the structure response and application of the numerical-experimental identification technique.

Mixed numerical-experimental methods are sensitive for model errors because the numerical model is always based on a series of hypotheses. If the real structure does not satisfy one or more of these hypotheses, the model of the structure is evidently not appropriate. Since the development of mixed numerical-experimental techniques for material identification is aimed at obtaining a practical method which yields quick and reliable results, much research has been done in order to minimize these model errors (see, e. g., Soares et al.; Frederiksen (1993; 1997b)).

In the meantime many different approaches were produced for identification of the physical parameters directly characterizing structural behavior (i.e. Young's modulus and density of the material). Bolognini et al. (1993) has performed appropriate comparison between actual eigenfrequencies of an existing structure and those obtained through the finite element analysis. It led to the identification of parameters which can be used for the model calibration as well as for the detection of damaged zones in the structure.

Numerical-experimental identification methods are mainly used in structural applications. For example, Soares et al. (1993) has identified elastic properties of laminated composites employing experimental eigenfrequencies. The stiffness parameters were identified from the measured natural frequencies of the laminated composite plate by direct

minimization of the identification functional. Similar approach was used by Frederiksen (1997a). For identification of elastic constants of the laminate Frederiksen (1997b) has employed an improved plate model. De Visscher et al. (1997) has shown that the mixed numerical-experimental method can be used for identification of damping properties of polymeric composites. Influence of modelling and measurement errors on parameter estimation was discussed in some papers (Frederiksen; Frederiksen (1997b; 1998)).

In the following the numerical-experimental method for the identification of mechanical properties of laminated polymeric composites from the experimental results of the structure response is described. The difference between conventional approach discussed by Soares et al. (1993) and the present approach is that instead of direct minimization of identification functional the experiment design is used, by which response surfaces of the functional to be minimized are obtained. The response surface approximations are obtained employing the information on the behavior of a structure in the sample points of the experiment design. Note that the finite element modeling of the structure is performed only in the sample points. The functional to be minimized describes the difference between the measured and numerically calculated parameters of the response of structure. By minimizing the functional the identification parameters are obtained.

The application of Response Surface Method (RSM) to design optimization and identification is aimed at reducing the cost of expensive analysis methods, e. g., finite element method. The main advantage of the present method is a significant reduction of the computational efforts. Previously the design of experiments and RSM was used for solution of the optimum design problems by Barthelemy and Haftka; Rikards; Rikards and Chate (1993; 1993; 1995). The response surface approach in different modifications was employed by many authors, e.g., Roux et al.; Toropov et al. (1998; 1998) and others. A review of optimization in relationship to experiment design was presented by Haftka et al. (1998).

The numerical-experimental method employed in the present study consists of the following stages. In the first stage the physical experiments are performed. Also the parameters to be identified, the domain of interest and criterion containing experimental data are selected. In the second stage the finite element method is used in order to model the response of the structure and calculations are performed in a sample points of the domain of interest. The sample points are determined by using a method of experiment design. In the third stage the numerical data obtained by the finite element solution in the sample points are employed in order to determine approximating functions (response surfaces) for a calculation of the structure response. In the fourth stage, using the approximating functions and experimentally measured values of the structural response, the identification of the material properties is performed. For this a corresponding functional is minimized employing methods of non-linear programming.

1.1 Parameters of Identification

Further it will be shown how the numerical-experimental approach is employed for identification of the elastic properties of laminated composite plates. It is assumed that the plate dimensions (see Fig. 1), plate mass, the layer angles β_i and the layer stacking sequence are known. Directions of material axes of a single layer are denoted 1-2-3, where

1 is the fiber direction and 2, 3 are the transverse directions (see Fig. 2). The unidirectional layer is assumed to be a homogeneous and transversely isotropic with respect to the fiber direction material. The goal is to identify the elastic properties of a single layer by measuring the response of laminated plate. For this a theory of composite laminates should be used. Modelling of laminates and laminated composite plates is outlined in textbooks (see, e.g., Jones; Altenbach et al.; Reddy (1975; 1996; 1996)).

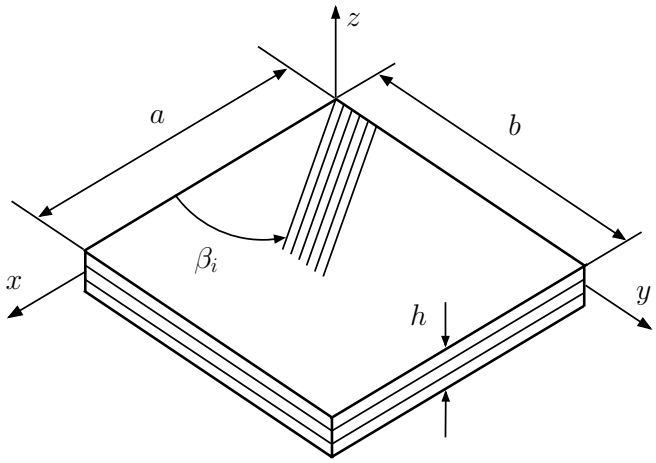

Figure 1. Geometry of laminated plate.

The parameters to be identified are five elastic constants of the single layer of the laminate: $E_1, E_2, G_{12}, G_{23}, \nu_{12}$. The laminated plate is modelled by the plate theory including transverse shear, rotatory inertia and extension of the normal line proposed by Rikards and Chate (1997). In this case the constitutive equation of the single layer of laminate in the symmetry axes of material is as follows

$$\begin{bmatrix} \sigma_{11} \\ \sigma_{22} \\ \sigma_{33} \\ \sigma_{23} \\ \sigma_{13} \\ \sigma_{12} \end{bmatrix} = \begin{bmatrix} A_{11} & A_{12} & A_{13} & 0 & 0 & 0 \\ A_{12} & A_{22} & A_{23} & 0 & 0 & 0 \\ A_{13} & A_{23} & A_{33} & 0 & 0 & 0 \\ 0 & 0 & 0 & A_{44} & 0 & 0 \\ 0 & 0 & 0 & 0 & A_{55} & 0 \\ 0 & 0 & 0 & 0 & 0 & A_{66} \end{bmatrix} \begin{bmatrix} \varepsilon_{11} \\ \varepsilon_{22} \\ \varepsilon_{33} \\ 2\varepsilon_{23} \\ 2\varepsilon_{13} \\ 2\varepsilon_{12} \end{bmatrix} \tag{1}$$

Here σ_{ij} is a stress tensor, ε_{ij} $(i, j = 1, 2, 3)$ is a strain tensor of the layer and A_{kl} $(k, l = 1, 2, ..., 6)$ is the elastic stiffnesses, which for the 3D stress state can be expressed through five elastic constants of the layer (see, e.g., Altenbach et al. (1996)). In the case of plane stress state these relations are as follows

$$A_{11} = \frac{E_1}{1 - \nu_{12}E_2/E_1}, \quad A_{22} = \frac{E_2}{1 - \nu_{12}E_2/E_1}, \quad A_{12} = \frac{\nu_{12}E_2}{1 - \nu_{12}E_2/E_1},$$

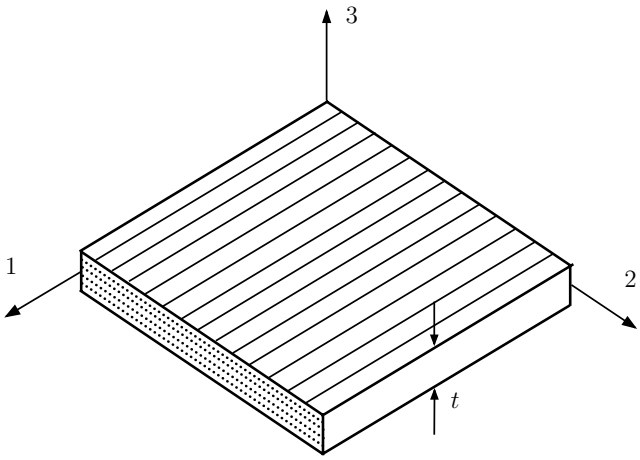

Figure 2. Single layer of laminated plate.

$$A_{44} = G_{23}, \quad A_{66} = G_{12} \tag{2}$$

Note that for transversely isotropic material $A_{22} = A_{33}, A_{12} = A_{13}, A_{55} = A_{66}$ and $A_{44} = 1/2(A_{22} - A_{23})$.

Laminated plates investigated here is of moderate thickness. For such plates influence of extension of the normal line on eigenfrequencies is negligible. Sufficient accuracy can be achieved employing a Mindlin's plate theory accounting for the transverse shear deformations only. However, for the Mindlin's plate theory in the constitutive equation (1) instead of stiffnesses A_{ij} a reduced stiffnesses Q_{ij} are used (see, e.g., Altenbach et al.; Reddy (1996; 1996)). In this case the reduced stiffnesses Q_{ij} are a non-linear functions of A_{ij}. The constitutive equation in form (1) is chosen to preserve linear dependence of the stiffness matrix of plate on parameters A_{ij}.

The plate is composed of unidirectionally reinforced layers. In general, the ith layer of the laminated plate can be oriented at an arbitrary angle β_i. The angles of the layers are assumed to be fixed. For example, the cross-ply laminate consists of the layers with angles $\beta_i = 0^0$ and $\beta_i = 90^0$.

The vector of parameters $\boldsymbol{x}$ to be identified can be chosen in a different ways. Components of this vector could be elastic engineering constants $E_1, E_2, G_{12}, G_{23}, \nu_{12}$ or elastic stiffnesses A_{ij}. The major problem in parameter estimation is ill-conditioning caused by unknown variables having substantially different order of magnitude. Sometimes the Young's modulus and Poisson's ratio can not be directly selected as components of vector $\boldsymbol{x}$ without proper scaling. The scaling by longitudinal modulus E_1 was employed by Frederiksen (1997c) and in addition a fixed scaling factor was chosen. Hence, all unknown parameters were measured on compatible scales. Similar scaling and reparametrisation was employed by Soares et al. (1993), where additional scaling by the first experimental frequency allows to reduce the number of unknown variables from five to four. Thus, ma-

terial parameters of the single layer can be expressed in terms of dimensionless variables α_i

$$\begin{aligned}
\alpha_2 &= 4 - 4\left(\frac{E_2}{E_1}\right), \\
\alpha_3 &= 1 + \frac{E_2}{E_1}(1 - 2\nu_{12}) - 4\left(\frac{G_{12}}{E_1}\right)\alpha_0, \\
\alpha_4 &= 1 + \frac{E_2}{E_1}(1 + 6\nu_{12}) - 4\left(\frac{G_{12}}{E_1}\right)\alpha_0, \\
\alpha_5 &= 4(G_{23} + G_{12})\frac{\alpha_0}{E_1}
\end{aligned} \tag{3}$$

where

$$\alpha_0 = 1 - \nu_{12}^2 \frac{E_2}{E_1} \tag{4}$$

The inverse relations of Eq. (3) are as follows

$$\begin{aligned}
\frac{E_2}{E_1} &= \frac{4 - \alpha_2}{4}, \\
\frac{G_{12}}{E_1} &= \frac{8 - \alpha_2 - 3\alpha_3 - \alpha_4}{16\alpha_0}, \\
\nu_{12} &= \frac{\alpha_4 - \alpha_3}{8 - 2\alpha_2}, \\
\frac{G_{23}}{E_1} &= \frac{2\alpha_5 - 0.5(8 - \alpha_2 - 3\alpha_3 - \alpha_4)}{8\alpha_0}
\end{aligned} \tag{5}$$

The variables α_i are chosen to be on compatible scales. The first set of identification variables is defined by these dimensionless quantities α_i. The vector $\boldsymbol{x}$ to be identified is given by

$$\boldsymbol{x} = [x_1, x_2, x_3, x_4] = [\alpha_2, \alpha_3, \alpha_4, \alpha_5] \tag{6}$$

Additional scaling parameter C was introduced using the first experimental frequency in order to eliminate one variable (see Soares et al. (1993)). Let the experimental angular eigenfrequencies be designated by $\bar{\omega}_1, \bar{\omega}_2, \ldots, \bar{\omega}_I$, where I is the number of measured eigenfrequencies $\bar{f}_i (\bar{\omega}_i = 2\pi\bar{f}_i)$. The corresponding numerical (predicted) eigenfrequencies f_i $(\omega_i = 2\pi f_i)$ for the set of material parameters α_i are represented by $\omega_1, \omega_2, \ldots, \omega_I$. Let us consider the scaling parameter C which is chosen according to the relation (see Soares et al. (1993))

$$C = \frac{\bar{\omega}_1^2}{\omega_1^2(E_1^0)} \tag{7}$$

where ω_1 is the first numerical eigenfrequency calculated with the prior selected longitudinal Young's modulus E_1^0 of the layer.

The second set of identification variables is defined by the stiffnesses A_{ij}. In this case the vector $\boldsymbol{x}$ is given by

$$\boldsymbol{x} = [x_1, x_2, x_3, x_4, x_5] = [A_{11}, A_{22}, A_{12}, A_{44}, A_{66}] \tag{8}$$

These parameters practically are to be on compatible scales. However, in order to obtain the engineering constants from A_{ij} in addition a system of three non-linear equations (2) should be solved.

Depending on minimization algorithm (see below) as components of the vector of identification variables can be directly chosen also the engineering elastic constants. This is a third set of identification variables $\boldsymbol{x}$ given by

$$\boldsymbol{x} = [x_1, x_2, x_3, x_4, x_5] = [E_1, E_2, G_{12}, G_{23}, \nu_{12}] \tag{9}$$

The elastic constants can be evaluated through the identification procedure using the experimental eigenfrequencies of the laminated composite rectangular plate of constant thickness h, length a and width b (see Fig. 1). Identification procedure can be formulated using either the vector of unknown variables (refeq4), (refeq4a) or (refeq4b). The selection depends on approximation method and minimization algorithm employed in identification (see below).

1.2 Identification functional

Firstly, the formulation of identification problem is given for the case if the vector of unknown variables is defined by Eq. (6).

The functional to be minimized describes deviation between the measured $\bar{\omega}_i$ and numerically calculated $\omega_i(\boldsymbol{x})$ frequencies (see Soares et al. (1993))

$$\Phi(\boldsymbol{x}) = \sum_{i=2}^{I} w_i \frac{(\bar{\omega}_i^2 - C[\omega_i(\boldsymbol{x})]^2)^2}{\bar{\omega}_i^4} = \sum_{i=2}^{I} w_i e_i^2 \tag{10}$$

Here e_i is relative discrepancy or residual and w_i are weights for identification functional using the first set of variables. It is possible of assigning non-negative weights to each residual. For simplicity, only unity values are used hereafter. The estimation can be based on any set of frequencies by assigning weights of zeros and ones as appropriate.

The identification of the elastic constants $\boldsymbol{x}$ is performed on the basis of information obtained from the measurements of the I lowest frequencies. Note that the first frequency is not directly used for identification since this frequency was used for the scaling (see Eq. (7)). The identification problem is formulated as follows.

$$\min_{\boldsymbol{x}} \ \Phi(\boldsymbol{x}) \tag{11}$$

Subject to constrains

$$g_1(\boldsymbol{x}) = 4 - \alpha_2 > 0 \ \text{ or } \ \frac{E_2}{E_1} > 0 \tag{12}$$

$$g_2(\boldsymbol{x}) = \frac{8 - \alpha_2 - 3\alpha_3 - \alpha_4}{16\left[1 - \left(\dfrac{\alpha_4 - \alpha_3}{8 - 2\alpha_2}\right)^2 \left(\dfrac{4 - \alpha_2}{4}\right)\right]} > 0 \ \text{ or } \ \frac{G_{12}}{E_1} > 0 \tag{13}$$

$$g_3(\boldsymbol{x}) = \frac{2\alpha_5 - 0.5(8 - \alpha_2 - 3\alpha_3 - \alpha_4)}{8\left[1 - \left(\frac{\alpha_4 - \alpha_3}{8 - 2\alpha_2}\right)^2 \left(\frac{4 - \alpha_2}{4}\right)\right]} > 0 \quad \text{or} \quad \frac{G_{23}}{E_1} > 0 \tag{14}$$

$$g_4(\boldsymbol{x}) = -\left|\frac{\alpha_4 - \alpha_3}{8 - 2\alpha_2}\right| + \sqrt{\frac{4}{4 - \alpha_2}} > 0 \quad \text{or} \quad \sqrt{\frac{E_1}{E_2}} - |\nu_{12}| > 0 \tag{15}$$

$$\alpha_i^{\min} \le \alpha_i \le \alpha_i^{\max}, \quad i = 2, 3, 4, 5 \tag{16}$$

The upper $\alpha_i^{\max}$ and the lower $\alpha_i^{\min}$ bounds on the identification parameters can be chosen using preliminary information about the composite material. Constraints (12)-(15) denote conditions of a positive definiteness of the elasticity matrix.

In the second formulation of the identification problem the functional to be minimized is as follows

$$\Phi(\boldsymbol{x}) = \sum_{i=1}^{I} w_i^{(2)} \frac{(\bar{\omega}_i^2 - \omega_i(\boldsymbol{x})^2)^2}{\bar{\omega}_i^4} = \sum_{i=1}^{I} w_i e_i^2 \tag{17}$$

Here w_i are weights and $\lambda_i \boldsymbol{x}) = \omega_i(\boldsymbol{x})^2$ is an eigenvalue of the equation describing vibrations of the plate (see below). For this functional the second (refeq4a) or the third (refeq4b) set of variables $\boldsymbol{x}$ can be used. Again constrains for the upper and lower bounds on elastic constants are used and in addition constraints for positive definiteness of the elasticity matrix are employed

$$\begin{aligned} &g_1(\boldsymbol{x}) = A_{11} > 0, \quad g_2(\boldsymbol{x}) = A_{22} > 0, \\ &g_3(\boldsymbol{x}) = A_{11}A_{22} - A_{12}^2 > 0, \\ &g_4(\boldsymbol{x}) = A_{44} > 0, \quad g_5(\boldsymbol{x}) = A_{66} > 0 \end{aligned} \tag{18}$$

The functionals (10) and (17) have been employed for identification by Rikards et al. (2001), where instead of original functions the approximating functions were used for each frequency. Thus, in this formulation the approximations were performed for each frequency or eigenvalue. Employing the same functional (17) procedure of identification can be modified so, that approximation is performed not for each frequency but for the functional $\Phi(\boldsymbol{x})$. Thus, the function to be minimized is as follows

$$\Phi(x^j) = \left(\sum_{i=1}^{I} w_i \left(\frac{(2\pi f_i^{\exp})^2 - \lambda_i(x^j)}{(2\pi f_i^{\exp})^2}\right)^2\right)^m = \Phi_j \tag{19}$$

Here $\lambda_i(x^j)$ is calculated by FEM ith eigenvalue in a sample point $x^j = (E_1^j, E_2^j, G_{13}^j, G_{23}^j, \nu_{12}^j)$ of a 5-dimensional space of identification parameters, j is number of sample point (see below) of experiment design ($j = 1, 2, ...N$), N is a total number of sample points (number of runs) in experiment design, $m = 1, 1/2, 1/4$ or $1/8$. The number m is chosen to improve quality of approximation. The best results were obtained (see below) with m=1/2 and 1.

The objective functions (10),(17), (19) are relating to the error in natural frequencies. Such functions mostly are used for identification. However, sometimes, for example, in damage identification the frequencies are not enough sensitive to detect localization of the damage zones. In this case the vibration mode shapes as well as the mode curvatures can be used for identification. Thus, the mode shape error function Φ_1 can be defined as follows

$$\Phi_1(x) = \sum_{i=1}^{I} w_i \left[\phi_i^{exp} - \phi_i(x)\right]^T \left[\phi_i^{exp} - \phi_i(x)\right] \tag{20}$$

Here ϕ_i^{exp} is experimentally measured mode shape and $\phi_i(x)$ is numerical mode shape. Such error function was used by Chakraborty and Mukhopadhyay (2000), where only a subset of deflection mode shape displacements was considered.

1.3 Experimental frequencies

Here two types of laminated composite plates are considered - a cross-ply glass/epoxy plates and unidirectionally reinforced carbon/epoxy plates.

The glass/epoxy cross-ply laminated plates consisting of 8 unidirectional layers with a layer stacking sequence $[90/0/90/0]_s$ were tested. A geometric dimensions and density of plates are presented in Table 1. The eigenfrequencies of the test plates were measured by a real-time television (TV) holography. The samples were hung upon two threads in order to simulate free-free boundary conditions. The sample was located in front of the holographic testing device. A piezoelectric resonator (in the following called "sensor") was glued in one corner to excite the sample plate with increasing frequency. The sensor is of circular shape with a diameter 25 mm located at the coordinates $x = a - 12.5$ mm and $y = b - 12.5$ mm (see Fig. 5). Mass of the sensor is m_s= 3.5 g. Other details of experiment was described in Rikards et al. (2001).

Table 1. Parameters of cross-ply laminated glass/epoxy plates.

Sample	a, m	b, m	h, mm	ρ, kg/m^3
PU10	0.1401	0.1401	2.011	1850
PU11	0.1401	0.1401	1.981	1850

Experiments were performed for both plates considered (see Table 1) and about 20 flexural eigenfrequencies were measured. The mode shapes also were recognized in the experiment. In Table 2 the experimental plate flexural frequencies are presented. The quantity n denotes the number of nodal lines parallel to x direction and m denotes the number of nodal lines parallel to y direction (see Fig. 1). The mode shapes (nodal lines) for the plate PU10 are presented in Fig. 3. Note that in Fig. 3 x is horizontal axis and y is vertical axis. These mode shapes were recognized in the experiment and most of them were used in identification. However prior to experiment the mode shapes

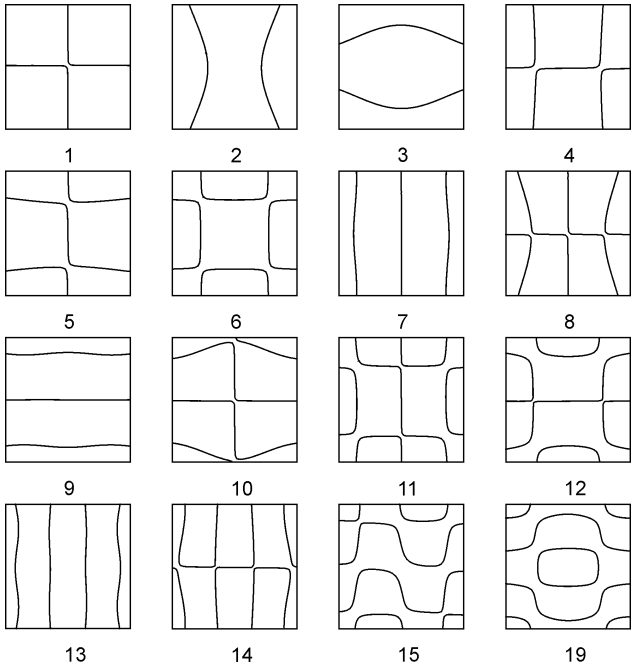

Figure 3. Vibration modes (m, n) of cross-ply laminated plate PU10.

were calculated by the finite element method using the initial guess values of the elastic constants. Such calculations is necessary in order to recognize all frequencies in the range and corresponding mode shapes. In calculations of the present mode shapes the mass of sensor was not taken into account. Calculating the plate with sensor the frequencies are slightly different and the mode shapes are similar but no more symmetric. Note that in the identification procedure each experimental frequency should be related to the numerical frequency having the same mode shape.

Carbon/epoxy unidirectionally reinforced plates. Similar experiments have been performed on unidirectional carbon/epoxy laminated plates (see Fig 4). Again plates were tested for vibrations in order to measure eigenfrequencies and corresponding modes. Experiments were performed with free-free boundary conditions on all edges of the plate in order to exclude influence of boundary conditions to the results of identification.

At all seven carbon/epoxy plates were tested. Fiber volume content of the carbon/epoxy laminate was about 60%. Nominal thickness of the plates was $h = 2$ mm (16 layer plates with a layer stacking sequence $[0_8]_s$) and $h = 6$ mm (48 layer plates with a layer stacking sequence $[0_{24}]_s$). The thick plates ($h = 6$ mm) were investigated in order to identify more accurate a transverse shear modulus. Geometric dimensions of all specimens are presented in Table 3.

Table 2. Experimental frequencies $\bar{f}_i^{exp}$ [Hz] of glass/epoxy plates.

Mode	Mode shape	Specimens	
i	m, n	PU10	PU11
1	1, 1	166	159
2	2, 0	341	332
3	0, 2	–	–
4	2, 1	484	464
5	1, 2	542	529
6	2, 2	902	869
7	3, 0	971	938
8	3, 1	1090	1050
9	0, 3	1155	1143
10	1, 3	1273	1240
11	3, 2	1523	1470
12	2, 3	1643	–
13	4, 0	1898	1838
14	4, 1	2003	1940
15	3, 3	2290	2180
16	0, 4	–	–
17	4, 2	2418	2338
18	1, 4	–	–
19	2, 4	2733	2665
20	4, 3	–	–
21	5, 0	3108	3023
22	5, 1	3233	3135
23	3, 4	–	–
24	5, 2	3605	–

Table 3. Geometric dimensions and density of carbon/epoxy plates.

Plate No.	a, mm	b, mm	h, mm	ρ, kg/mm^3
ud1	207.5	207.5	2.000	1535
ud2	205	205	2.000	1562
ud3	205	205	1.969	1598
ud4	205	210	1.998	1533
ud5	205	205	1.960	1589
ud6	205	212.5	6.081	1472
ud7	202.5	200	6.126	1576

Experimental eigenfrequencies and eigenmodes of carbon/epoxy unidirectionally reinforced plates are presented in Table 4. Since all frequencies experimentally were not observed, frequencies are ranged according to the finite element solution employing the initial guess values of elastic constants obtained from the static tests. In the second column corresponding vibration modes (n, m) are given, where n is number of nodal lines

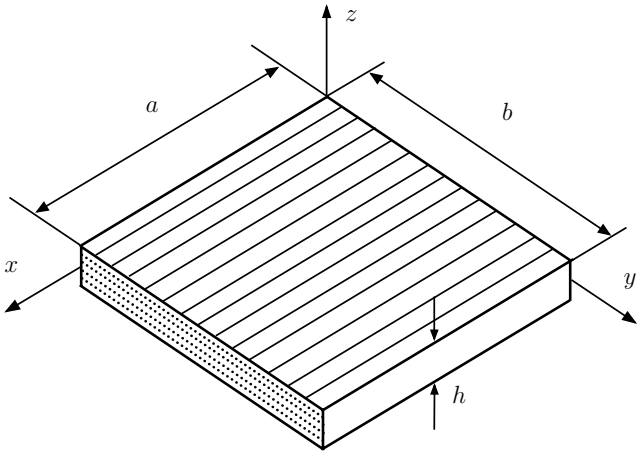

Figure 4. Unidirectionally reinforced carbon/epoxy plate.

parallel to x axis and m is number of nodal lines parallel to y axis. Note that axis x is in the fiber direction and axis y is in the transverse direction. It is seen that in the experiment all frequencies were not observed. For example, for the plate UD1 in the range of first 18 numerical frequencies only 12 experimental frequencies were measured.

Table 4. Experimental frequencies $\bar{f}_i^{exp}$ [Hz] of carbon/epoxy plates.

No.	n, m	UD1	UD2	UD3	UD4	UD5	UD6	UD7
1	1, 1	97	97.6	98.2	97.5	98	299.5	299
2	2, 0	123.8	123.4	126	125	127	377	377.5
3	2, 1	237.4	245	237	236	238	721	720.5
4	3, 0	341	342	345.6	344	350	1047	1046
5	3, 1	458	–	457	457.5	458	1396	1388
6	0, 2	502.6	501	498	497	496	1520.5	1512
7	1, 2	541.2	538	536.5	537.5	533	1636.5	1630.5
8	2, 2	653	653	654	650	649	1968	1959
9	4, 0	–	–	–	682.5	–	2051	–
10	4, 1	–	–	780	784	–	2360	–
11	3, 2	–	866	863	866	858	2580	2569
12	5, 0	–	1124.5	1125	1124.5	–	–	3370
13	4, 2	1168	–	–	–	–	–	–
14	5, 1	–	–	1242	–	–	–	–
15	0, 3	1381	–	1368.5	1365.5	1355	4042	4032.5
16	1, 3	1413	–	1401.6	1402.5	1391	4145	4141
17	2, 3	1512	–	1506.5	1504	1487	4410	4386
18	5, 2	–	1589	–	–	–	–	–

Experimental frequencies presented in Tables 3 and 4 will be used in identification of elastic constants for a single layer of the cross-ply glass/epoxy plates and for the unidirectionally reinforced carbon/epoxy plates (see below).

1.4 Finite element model

The eigenvalue problem for harmonic vibrations of the plate can be represented by

$$\boldsymbol{K}(x)\boldsymbol{u} = \lambda(x)\boldsymbol{M}\boldsymbol{u} \tag{21}$$

Here $\boldsymbol{K}(x)$ is the stiffness matrix of the plate, $\boldsymbol{M}$ is the mass matrix, $\boldsymbol{u}$ is the displacement vector and $\lambda(x) = \omega^2(x)$ is eigenvalue. Note that circular frequency $\omega = 2\pi f$, where f is eigenfrequency. The eigenvalue relation (21) for the mode $\boldsymbol{u}_1$ which corresponds to the first experimental eigenfrequency $\omega_1^{exp} = \bar{\omega}_1$ can be written in an equivalent form placing E_1 in evidence

$$E_1\boldsymbol{K}^*\boldsymbol{u}_1 = \bar{\omega}_1^2\boldsymbol{M}\boldsymbol{u}_1 \tag{22}$$

Here $E_1\boldsymbol{K}^* = \boldsymbol{K}$ is the stiffness matrix. Taking into account relation (7) this equation can be written as

$$CE_1^0\boldsymbol{K}^*\boldsymbol{u}_1 = C\omega_1^2\boldsymbol{M}\boldsymbol{u}_1 \tag{23}$$

hence

$$E_1 = CE_1^0 \tag{24}$$

where E_1^0 is the initial guess value given to the Young's modulus in the fiber direction of the layer and E_1 is the corresponding identified mechanical property. After evaluation of the optimum value of x for the first set of identification variables the remaining mechanical properties are calculated by inverse relations (5).

For the second or third set of identification variables x the same eigenvalue equation (21) has been solved. The only difference is that other reference points of experiment design (see below) are selected since in this case the dimension of the design space is five. Hence numerical frequencies are predicted in other points of the design space as in the case of using the first set of design variables, for which the dimension of the design space is four.

The eigenvalue problem (21) was solved by using subspace iteration technique (see Bathe (1982)) and a triangular finite element of laminated thick plate with a shear correction (see Rikards and Chate (1997)). In order to avoid 'shear locking' a selective integration technique was applied. A 22×22 regular mesh (968 finite elements) was considered in order to achieve appropriate accuracy for at least 20 first eigenvalues of the laminated plate with FFFF (all edges free) boundary conditions. The finite element mesh of the plate is shown in Fig. 5. In calculations of predicted frequencies $\omega(x)$ for the cross-ply glass epoxy plates the mass of sensor should be taken into account. For the carbon/epoxy plates other experimental technique has been used without sensor. In this case there is no additional mass on the plate.

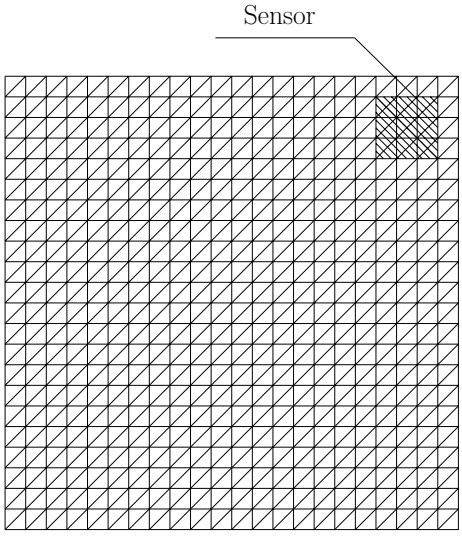

Figure 5. Finite element mesh.

1.5 Experiment Design and Approximation

Important for identification is the problem of minimization of identification functionals (10), (17) or (19). Here the method of experiment design and response surface method is used to solve the minimization problem.

In order to reduce computational efforts firstly the methods based on approximation concepts have been used in structural optimization (see, e.g., Barthelemy and Haftka (1993)). The development of approximation functions has become a separate problem in optimum structural design, which was discussed by Toropov (1989). The approximating models can be built in different ways. Empirical model building theory was developed by Box and Draper (1987). To construct a more general model of the original function the method of experiment design (Audze and Eglais; Haftka et al. (1977; 1998)) together with approximate model building (Eglais; Meyer et al.; Khuri and Cornell (1981; 1995; 1996)) can be employed. A simplified model, called metamodel, is built using results of a numerical experiment in a sample points of experiment design. Response analysis using the simplified model is computationally much less expensive than solution employing the original model. Although there is a wide literature about experiment design and building of approximating functions it should be noted that there are some special features present in experiment design but not present in the physical experiment. Below some problems of experiment design are discussed.

There are two cases of building the approximating functions. The first situation is that deterministic computer simulation is presented only. Such case was discussed in investigations related to solution of structural optimization problems (see, e.g., Barthelemy and Haftka; Toropov (1993; 1989)). Deterministic computer simulation was employed

also to build the approximating functions for solution of identification problems (Rikards et al.; Rikards et al. (1999; 2001)). However, in identification problems also a physical experiment is presented. In the previous investigations (Rikards et al.; Rikards et al. (1999; 2001)) a physical experiment was not used to build the approximating functions. Then the experimental values was employed only for identification purposes. However, it is possible to combine data from both computer and physical experiments. This is a second situation, in which both the data from computer experiments as well as from related physical experiments for the same factor and related response variables have been employed. Traditional statistical approaches consider each of these sets of data (computer and physical experimental data) separately with corresponding separate analyses and fitted statistical models. However, it is possible simultaneously analyze the combined data using, for example, hierarchical Bayesian integrated modeling approach. Simultaneous analysis of such combined data permits the unknown coefficients in response surface model to be more precisely estimated, thereby producing a better fitting response surface. Although the problem of identification discussed in the present paper belongs to the combined data set, here the approximating functions are built employing the combined data set as well as the deterministic computer simulation.

Computer models are often used to perform experiments before expensive physical experiments are performed. The main features of deterministic computer simulation are as follows.

- The results obtained in the numerical experiment are deterministic without a statistical error. Repetition of the results is 100%. It means that there is no statistical dispersion of the model parameters. However, computer models produce numerical noise as a result of the incomplete convergence of iterative processes, round-off errors, and the discrete representation of continuous physical phenomena, when different number of calculation steps or a different finite element grid being generated (see, e.g., Giunta et al. (1994)). In deterministic computer experiments, replication at a sample point is meaningless; therefore, the points should be chosen to fill the design space.
- Mathematical model of the object is unknown, i.e. the form of the regression equation is not known. Therefore, the well-known criteria for experiment design optimality, for example, D-optimality, cannot be used. Such criteria can be used only in the case, when the form of regression equation is known.

There is wide literature about different methods of experiment design. Among the methods specially can be emphasized the space filling designs. The first space filling design for computer experiment was proposed by Audze and Eglais (1977). Here firstly the designs in which the number of levels for each variable is equal to the total number of runs were proposed. Eglais has firstly used also the space filling criterion for such designs based on function similar to potential energy of gravity. Later the same kind of experimental designs was proposed as a Monte Carlo integration technique by McKay et al. (1979) and the name Latin hypercube samplings was introduced. Numerous space filling experimental designs have been developed in an effort to provide more efficient and effective means for sampling deterministic computer experiments based on Latin hypercubes. Later a lot of space filling criteria for Latin hypercube designs was proposed by many

authors: Maximin Latin hypercubes by Johnson et al. (1990), Minimal Integrated Mean Squared Error designs by Sacks et al. (1989), Orthogonal array-based Latin hypercube designs by Tang (1993), Orthogonal Latin hypercubes by Ye (1998), Integrated Mean Squared Error (IMSE) optimal Latin hypercubes by Park (1994).

The approach of experiment design and approximation proposed by Eglais can give good results for the problems based on numerical experiment (Audze and Eglais; Eglais (1977; 1981)). This approach based on global approximation was employed for solution of identification problems (Rikards et al.; Rikards et al. (1999; 2001)). However, sometimes the results of the approximation are not satisfactory. It will be shown below that the accuracy of solution can be improved by using a minimal Mean Square Distance (MSD) design and a local approximation method to solve similar identification problem.

In the last years the so-called non-parametric approximation methods becoming widely used for the design and analysis of computer experiments: local polynomial approximation (Cleveland and Devlin; Koehler and Owen (1988; 1996)) and Kriging (Sacks et al. (1989)). Finally, other statistical techniques such as Multivariate Adaptive Regression Splines (Frederiksen (1998)) and Radial Basis Functions (Hardy; Dyn et al.; Powell (1971; 1986; 1987)) are beginning to draw the attention of many researchers. However, these methods are computationally expensive not only for metamodel building, but also for using of metamodels for prediction.

The stages of solution of identification problem considered here are as follows.

- Development of finite element model to perform deterministic computer experiments.
- Formulation of identification functional and selection of variables to be identified.
- Performing the physical experiment.
- Elaboration of experiment designs to determine a sample points in which deterministic computer simulation is performed.
- Deterministic computer simulation in the sample points of experiment design.
- Building the approximating function (global or local approximations) employing the data set of deterministic computer experiment (alternative - employing a combined data set of numerical and physical experimental data).
- Minimization of functional.
- Verification and validation of results.

1.6 Latin Hypercube Designs

In previous section different experiment designs used for the model building were reviewed. The choice of the design of experiments can have a large influence on the accuracy of the approximation and the cost of constructing the response surface. In order to solve the present identification problem two types of experiment designs are employed - the Latin Hypercube Design (LHD) and the Minimal Mean Squared Distance (MMSD) design.

Latin Hypercube Design proposed by Audze and Eglais (1977) and McKay et al. (1979) can be viewed as an N-dimensional extension of Latin square design. The main feature of LHD is that on each level of every design variable only one point is placed. There are the same number of levels as runs (number of points of experiment or number

of sample points). McKay et al. (1979) has proposed that levels are assigned randomly to runs. Other criterion was proposed by Audze and Eglais (1977). Here this criterion will be explained in details.

Audze and Eglais (1977) proposed a non-conventional criterion for elaboration of experiment designs which is not dependent on the mathematical model (approximating functions) of the problem under consideration. The input data for the elaboration of the plan include only the number of variables N (number of factors) and the number of experiments K. The main principles in this approach are as follows.

1. The number of levels of factors (same for each factor) is equal to the number of experiments and for each level there is only one experiment. This is similar to LHD proposed by McKay et al. (1979).
2. The sample points (points of experiment) are distributed as regular as possible in the domain of variables.

To realize the second principle it is suggested to use a criterion

$$\Psi = \sum_{i=1}^{K-1} \sum_{j=i+1}^{K} \frac{1}{L_{ij}^2} \Rightarrow \min \tag{25}$$

where L_{ij} is a distance between the reference points having numbers i and j ($i \neq j$). The criterion (25) is a physical analogy of the minimum of potential energy of repulsive forces for a set of points of unit mass, if the magnitude of these repulsive forces is inversely proportional to the distance L_{ij} cubed between the points. Note that the force can be obtained as derivative of the potential energy.

The problem of minimizing the criterion (25) together with the first principle leads to a non-linear programming problem. Solving the non-linear programming problem the experiment designs (plans) can be determined for different number of the design variables N and different number of sample points K (runs).

The elaboration of the plans is time consuming, so each plan of experiment is elaborated only once and stored in a matrix characterized by the level of factors for each of K experiments. For example, for a number of factors (design variables) $N = 2$ and $K = 9$ the matrix is given by

$$\boldsymbol{B}^T = \begin{bmatrix} 7\,1\,2\,5\,4\,9\,6\,8\,3 \\ 2\,6\,3\,5\,1\,4\,9\,7\,8 \end{bmatrix} \tag{26}$$

The corresponding plan of experiments is shown in Fig. 6. The domain of interest (domain of variables) is determined as $x_j \in [x_j^{\min}, x_j^{\max}]$, where $x_j^{\min}$ and $x_j^{\max}$ are respectively the lower and the upper bounds on the design variables. Thus, in this domain the sample points, where the numerical experiments must be performed, are calculated by the expression

$$x_j^{(i)} = x_j^{\min} + \frac{1}{K-1}(x_j^{\max} - x_j^{\min})(B_{ij} - 1) \tag{27}$$

Here $i = 1, 2, ..., K$ and $j = 1, 2, ..., N$. Since the matrices B_{ij} of the experiment design are universal, they may be used for the various identification or optimum design problems.

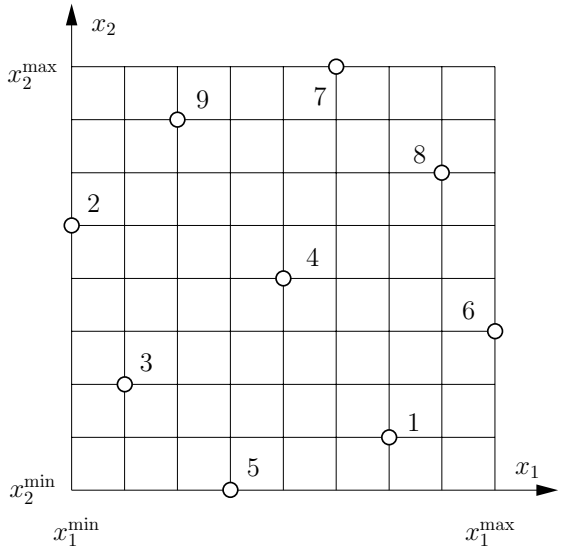

Figure 6. Eglais' design for $N = 2$ and $K = 9$

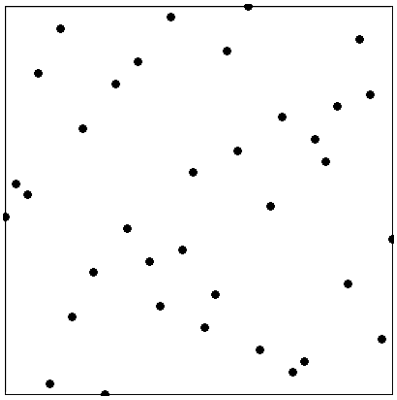

Figure 7. View of Eglais' design in plane 1-2 for $N = 5$, $K = 36$ and $\Gamma = 3322$.

Problem of identification of elastic constants (five variables) was solved employing Eglais' experimental designs. A 36-point 5-dimensional experiment design is shown in Fig. 7.

Eglais' designs can be evalueted also by other criterions. Such criterions can be chosen evaluating possible error of approximation. Knowing that in approximation it will be necessary to obtain the values of interpolated function in the points of the s-dimensional grid, it is essential that points of initial experiment are distributed so, that locally ap-

proximated values will be as accurate as possible. By performing approximation with the second order polynomials, the error of interpolation is increasing proportionally to the product of distance between the points used in interpolation, if the points are distributed close enough. In the neighborhood of the grid point, there are only few points of the real experiment (usually only one to two points). Therefore, the quality of experiment design is characterized by a sum of the distance between all grid points and the closest experimental point raised to the power of four

$$\Gamma = \sum_{i=1}^{N_F} \Delta_i^4 \tag{28}$$

where Δ_i is the distance between the grid point z_i and the closest experimental point, $N_F = M^s$, $s = N$ is number of input variables, M is number of equidistant points for each input variable, for example, this value can be chosen $M = 7$. Using the criterion (28) the Eglais' designs can be evaluated. For example, for the 36-point design presented in Fig. 7 $\Gamma = 3322$.

Minimizing the criterion (28) new designs can be elaborated. The minimum of criterion without constraints can be easily found by employing the Newton's method. In Fig. 8 one projection of the 36-point five-dimensional experiment design is shown (the value of the cost function $\Gamma = 1739$ is the best that was found for this design). In Fig. 9 the experiment design optimized according to the criterion (28) is shown using as initial estimate the Eglais' design. It can be seen that the improvement is negligible in comparison with the original Eglais' design presented in Fig. 7. By distributing the levels of experiment regularly in the interval [-1,+1], but not requiring that extreme levels should be exactly at -1 and +1, a slightly better value of cost function $\Gamma = 3271$ was obtained. So, the Latin hypercube designs can be evaluated employing different criterions - Eqs. (25), (28) or others.

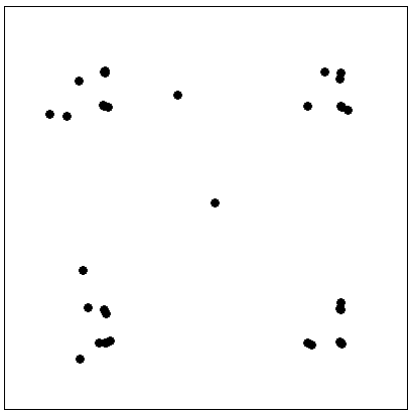

Figure 8. View of 5-dimensional 36-point design (28) in plane 1-2 with $\Gamma = 1739$.

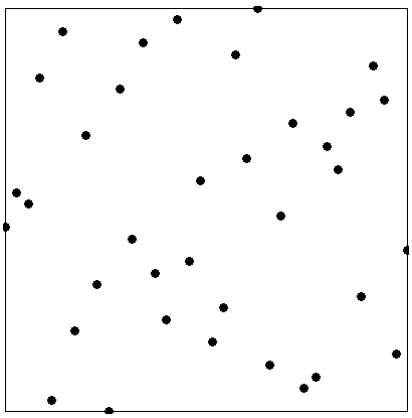

Figure 9. View of 5-dimensional 36-point Latin hypercube design optimized according (28) in plane 1-2 with $\Gamma = 3318$.

1.7 Minimal Mean Squared Distance Design

For the computer experiment a Minimal Mean Squared Distance (MMSD) experimental designs can be successfully employed. These designs were proposed by Auzins and Janushevskis (2002). The MMSD designs are space filling designs, which gives minimal Mean Squared Distance (MSD) between points in design space R and nearest point from experimental design D

$$MSD = \sqrt{\left(\frac{1}{n}\right)\sum_{v=1}^{n}\min_{u=1,\ldots,N}\left[\sum_{i=1}^{m}(w_{iv}-x_{iu})^2\right]} \tag{29}$$

where w_v is a large sample from the points in design space R ($v = 1, ..., n$). Hereafter about 1000000 equidistant mesh points for low dimensions ($m = 2, 3$) are employed and a 100000 Latin hypercube sample for large-scale designs ($m > 3$) are used. These designs give points uniformly distributed in design space and tend to minimize the expected mean squared error of local quadratic approximation Auzins and Janushevskis (2002). Fang and Wang (1994) introduced similar criterion, named Mean Squared Error. In (Auzins and Janushevskis (2002)) a quick search algorithm for minimization of MSD criterion for Latin hypercube designs in the unit cube $[-1, 1]^m$ as well as for designs with unconstrained level values and numbers in unit cubes or m-dimensional spherical regions was proposed.

For illustration of MSD design search algorithm a 6-point experimental design in two dimensions is shown in Fig. 10. A 33×33 regular grid with 1089 equidistant mesh points are employed. The functional (29) is minimized in the following steps. In the first step a sample points is distributed randomly in the design space. Then each mesh

point is related to the closest sample point. In Fig. 10 the grid points related to the same sample point are marked with the same color. Further for the grid points with the "same color" the criterion (29) is minimized. Then again each mesh point is related to the closest sample point and iteration is continued. In about 5-6 iterations the optimum distribution of sample points is found. In Fig. 10 the distribution of sample points after four iterations is shown. The final (optimum) distribution is shown in Fig. 11.

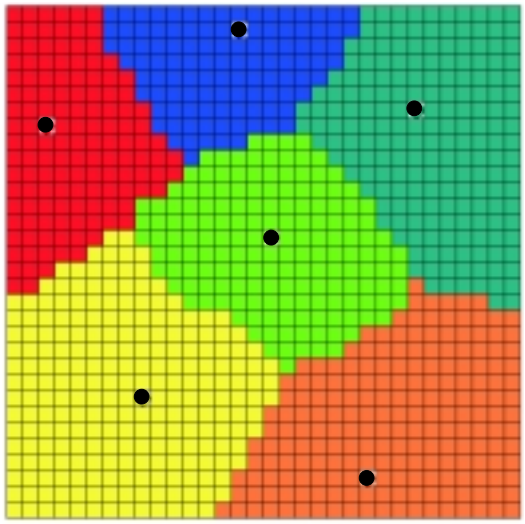

Figure 10. Iteration procedure for 6-point two dimensional MSD design.

For the purpose of comparing with other designs throughout this paper distances and others characteristics of experimental designs are computed after designs are scaled into the unit cube $[0,1]^m$ although the designs are mostly constructed in m-dimensional cube $[-1,1]^m$. For comparing with other space filling designs four additional criterions have been used.

1. The Eglais' criterion (Audze and Eglais (1977)), later proposed also by Morris and Mitchell (1995) in more general form

$$\Phi_2 = \left[\sum_{u=1}^{K-1} \sum_{v=u+1}^{K} \frac{1}{\sum_{i=1}^{m} (x_{iu} - x_{iv})^2} \right]^{1/2} \tag{30}$$

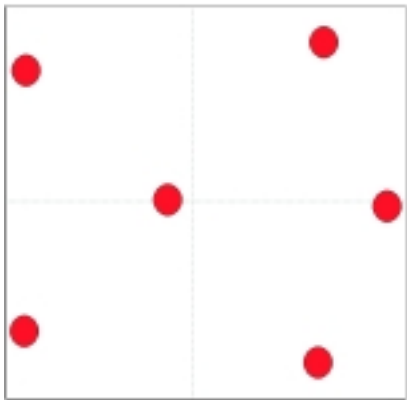

Figure 11. Optimum according criterion (29) 6-point two dimensional MSD design.

2. The MINDIST criterion, which seeks to maximize the minimum distance between any pair of points in the data collection plan (see Johnson et al. (1990))

$$\text{MINDIST} = \min_{u,v=1,\ldots,N} \sum_{i=1}^{m} (x_{iu} - x_{iv})^2 \tag{31}$$

3. The entropy criterion, first proposed by Shewry and Wynn (1987) and then adopted by Currin et al. (1991). The entropy criterion for designs in unit cube $[0,1]^m$ is equivalent to the minimization of $-\log|\mathbf{C}|$, where C is the $N \times N$ covariance matrix of the design with elements

$$c_{ij} = \exp\left\{-\Theta \sum_{k=1}^{m} |x_{ki} - x_{kj}|^q\right\}, 0 < q \leq 2 \tag{32}$$

where $i, j = 1, , N$. Throughout this paper the value $q = 2$ is selected so, that the correlation between two points is a function of their Euclidean distance L_2, and Θ is set equal to 2.

4. The discrepancy criterion (Palmer and Tsui (2001)), which averages the squared difference in the cumulative density function

$$\begin{aligned}(D_C)^2 = &\left(\frac{13}{12}\right)^m - \frac{2}{N}\sum_{u=1}^{N}\prod_{i=1}^{m}\left[1 + 0.5\,|x_{iu} - 0.5| - 0.5\,|x_{iu} - 0.5|^2\right] \\ &+\frac{1}{N^2}\sum_{u=1}^{N}\sum_{v=1}^{N}\prod_{i=1}^{m}\left[1 + 0.5\,|x_{iu} - 0.5| + 0.5\,|x_{iv} - 0.5| - 0.5\,|x_{iu} - x_{iv}|\right]\end{aligned} \tag{33}$$

Experimental designs have been compared by using these different criterions. Table 5 shows comparison of three 16-run designs of 7 variables for five criterions. The MMSDLH means Minimal MSD Latin Hypercube design, the ULH means Uniform Design Based

Table 5. Comparison of 16 sample point designs for 7 variables.

Design	MSD	Φ_2	MINDIST	Entropy	D_C
MMSDLH	0.3942	9.5196	0.8869	0.2900	0.2464
ULH	0.4006	9.5449	0.8353	0.3123	0.2289
MBLH	0.3947	9.5281	0.8000	0.3147	0.2468

on centered L_2 discrepancy $U_n(n^s)$ (see Fang et al. (1999)) and MBLH is a Minimum Bias Latin hypercube design (see Palmer and Tsui (2001)).

The MMSDLH plan performs better than the others according to all five criterions. For the problem of identification of elastic constants of carbon/epoxy plates formulated above the MMSDLH type design with 101 runs and 5 factors is employed. For this design the values of criterions are as follows: MSD=0.2051, $\Phi_2 = 89.0740$, MINDIST=0.3808, Entropy=69.7806, $D_C = 0.0453$.

1.8 Global approximations

The next step after design of experiment is model building. As it was mentioned above the response surface methodology (RSM) is a collection of mathematical and statistical techniques for empirical model building. Originally, RSM was developed to model experimental responses, and then migrated into the modelling of numerical experiments. The difference is in type of error generated by the response. In physical experiments inaccuracy can be due, for example, to measurement errors, while in computer experiments numerical noise is a result of incomplete convergence of iterative processes, round-off errors or the discrete representation of of continuous physical phenomena.

Mainly simulation is performed by a computer analysis code. The basic approach is to construct approximations of the analysis codes to get the functional relationship between x and y. Here x is design variables (inputs) and y is response (output). If the true nature of a computer analysis code (original function) is represented as

$$y = f(x) \tag{34}$$

then the approximation or metamodel ("model of the model") of the original function is taken to be

$$\hat{y} = g(x), \quad y = \hat{y} + \varepsilon \tag{35}$$

where ε represents both the error of approximation and measurement or random errors. Above we have discussed how to choose efficient set of sample points $(x_1, x_2, ..., x_n)$. Having this information the regression analysis can be performed to create global or local approximations. These approximations then can replace the existing computer code (original function).

Example of Response Surface. Let us consider approximation of the second eigenfrequency f_2 of the plate UD7. The design variables were defined by Eq. (9)

$$x = [x_1, x_2, x_3, x_4, x_5] = [E_1, E_2, G_{12}, G_{23}, \nu_{12}] \tag{36}$$

Employing the MMSDLH type 101-point design in five dimensional space the eigenfrequencies according Eq. (21) were calculated by FEM using own programme. These eigenfrequencies obtained by the software code is original function. Calculations were performed in a sample points of experiment design. These sample points are distributed in the domain of interest, which is formed by lower and upper limits of variables

$$x_i^{\min} \leq x_i \leq x_i^{\max} \tag{37}$$

The second eigenfrequency f_2 (original function) is a function of all five design variables and approximating function $\hat{f}_2$ is given by

$$f_2 = \hat{f}_2(x_1, x_2, x_3, x_4, x_5) + \varepsilon \tag{38}$$

where ε represents the error of approximation of the original function f_2. The surface represented by $\hat{f}_2(x_1, x_2, x_3, x_4, x_5)$ is called a response surface.

The response surface can be represented graphically. In Fig. 12 a three-dimensional response surface is presented as function of two (transverse shear modulus G_{23} and Poisson's ratio ν_{12}) of five design variables.

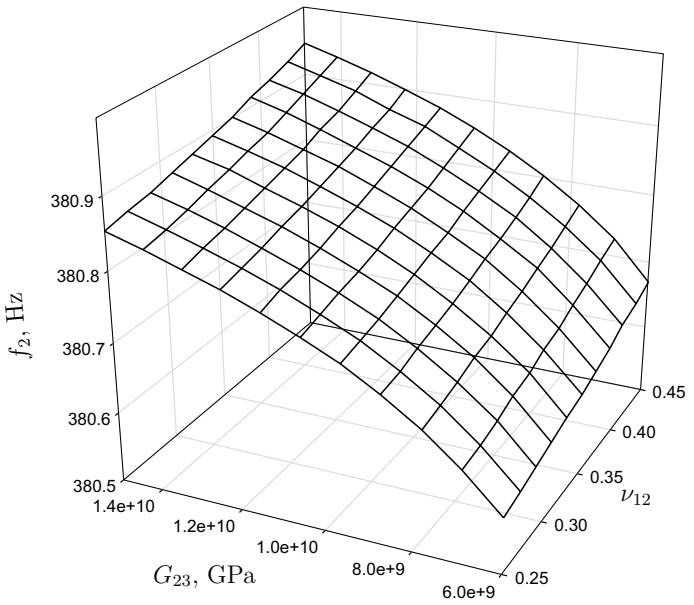

Figure 12. Three-dimensional response surface for second eigenfrequency of plate UD7.

The response surface can be represented graphically also as contour plot that help visualize the shape of the response surface. Contours are curves of constant response

drawn in the $x_i,\ x_j$ plane keeping all other variables fixed. Each contour corresponds to a particular height of the response surface as shown in Fig. 13, where the contour plot of Eq. (17) is presented.

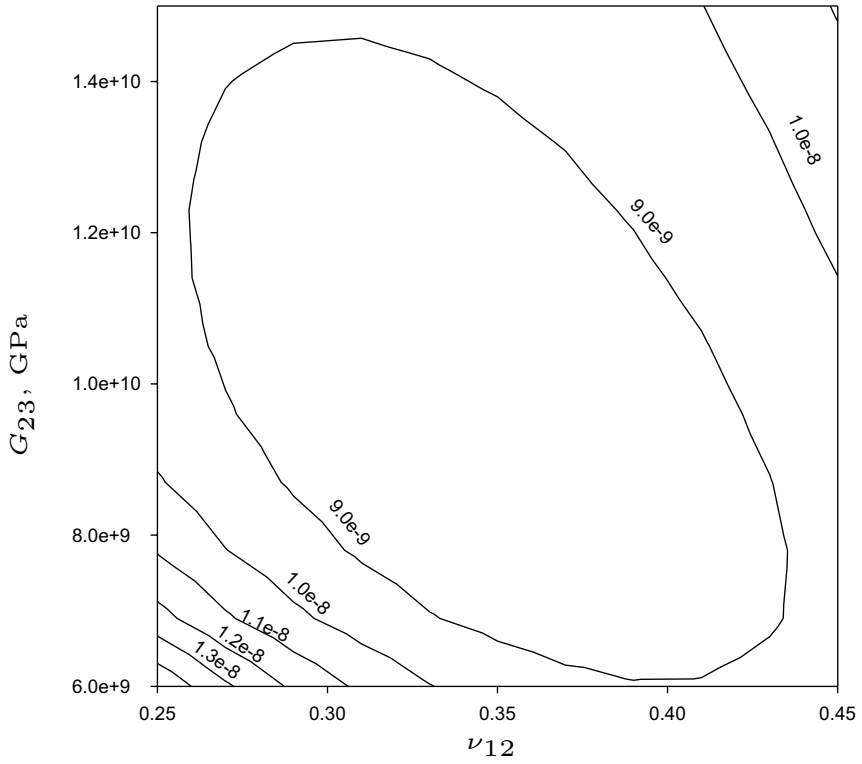

Figure 13. Contour plot of the discrepancy functional (17).

Generally, the structure of the relationship between the response and the independent variables is unknown. The first step in RSM is to find a suitable approximation to the true relationship. The most common forms are low-order polynomials (first or second-order).

The existing methods of regression analysis are based on the principle that the equation form is *a priori* known and the problem is to find coefficients (the so called tuning parameters) of the equation. However, in most cases the form of the equation also must be determined. Such a method was proposed by Eglais (1981) and he developed also the programme RESINT. This code was employed for obtaining the response surfaces for

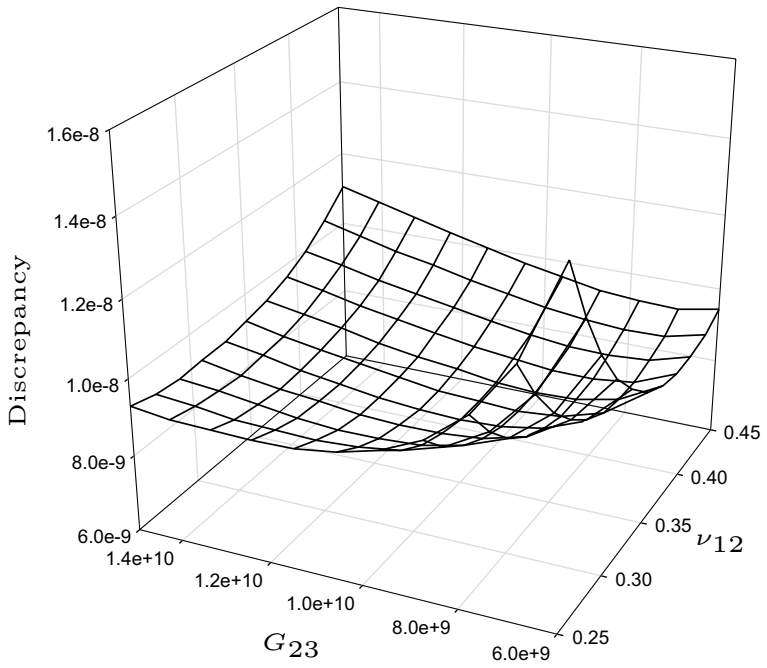

Figure 14. Three-dimensional response surface for discrepancy functional (17).

the structural optimization problems (Rikards; Rikards and Chate (1993; 1995)). Further this method is briefly outlined.

Building a Model by Software Code RESINT. Let us consider a method, in which a form of the regression equation is unknown. There are two requirements for the regression equation - accuracy and reliability. Accuracy is characterized by a minimum of standard deviation. Increasing the number of terms in the regression equation (response surface) could improve accuracy, moreover, it is possible to obtain a complete agreement between the experimental data and values given by the equation of regression. But in this case the prediction can be very poor at the other points of the domain of interest. Reliability of the regression equation means that accuracy for the reference points and any other point in the domain of interest is approximately the same. Obviously, if the number of terms of the regression equation decreases, the reliability of the model increases. A compromise between accuracy and reliability of the model must be found. To realize these principles different approaches have been proposed. For example, Toropov et al. (1998) has proposed the algorithm where the approximating function was built using genetic

programming. The quality of approximation was measured by the fitness function and special coefficient penalizing the excessive length of the expression was introduced.

In the code RESINT the selection of the 'best' regression equation (response surface) in the subregion defined by the lower and upper bounds on the design variables is performed by the following procedure. The response surface is built by using data obtained by computer simulation in all points of experiment design. First, consider the approximating function (model) of the following form

$$\hat{y}(x) = \sum_{i=1}^{m} A_i \phi_i(x) \tag{39}$$

where A_i are unknown coefficients (tuning parameters) and $\phi_i(x)$ are the functions that constitute the model. These functions are built from the set of simple functions $\varphi_1, \varphi_2, \ldots, \varphi_R$. The functions φ_r $(r = 1, 2, \ldots, R)$ are assumed to be in the form

$$\varphi_r(x) = \prod_{j=1}^{n} x_j^{\alpha_{rj}} \tag{40}$$

where n is the number of variables and α_{rj} are positive or negative including zero integers. The form of the approximating function (39) is determined in two steps. First, the perspective functions $\phi_i(x)$ are selected by using the least-squares estimation. Then a step-by-step reduction procedure of the number of terms in the model is applied and further reduction of the selected functions is performed. In each step a new set of tuning parameters A_i is obtained. Details of this procedure and corresponding program RESINT were described by Eglais (1981) and also by Rikards (1993). The reduction procedure for one numerical example will be shown below in order to obtain the approximating function for the second eigenvalue of the equation (21) describing the vibrations of the cross-ply laminated plate (see Fig. 15). Note that there is no general rules for the procedure of reduction of terms in the model (response surface function) and it is necessary to acquire some experience to obtain appropriate function.

The approach outlined above is one possible method of global approximation. Other commonly used approximation method employed hereafter is fitting the response surfaces by polynomial functions.

1.9 Local Approximations and Minimization

The functionals Φ (Eqs. (10), (17) or (19)) can minimized employing a local approximation

$$\hat{\Phi}(x) = \beta_0 + \sum_{i=1}^{5} \beta_i x_i + \sum_{i=1}^{5} \sum_{k=i}^{5} \beta_{ik} x_i x_k \tag{41}$$

Here the lower index is used for the component of variable x_i $(i = 1, 2, .., 5)$, but upper index (see expression (17)) is employed to indicate the number of sample point in the

experiment design ($j = 1, 2, ...N$). In approximation (41) the coefficients are calculated by

$$\beta = \arg\min_{\beta} \sum_{j \in N_X} w(x - x_j) \left(\frac{\Phi_j - \beta_0 - \sum_{i=1}^{5} \beta_i x_{ji} - \sum_{i=1}^{5} \sum_{k=i}^{5} \beta_{ik} x_{ji} x_{jk}}{\Phi_j} \right)^2 \tag{42}$$

where $\beta_0, \beta_i, \beta_{ik}$ are coefficients of the local quadratic approximation, N_X is a set of numbers of the closest neighbors of the point x. Practically all points of experiment design are employed: $N_X = (1, 2, ..., N)$. In (42) $w(x - x_j) = \exp(-G \|x - x_j\|^2)$ is Gaussian weighting coefficient for the local approximation, $\|x - x_j\|$ is Euclidean distance between x and x_j, G is coefficient of Gaussian function. Usually it was taken $G = 0.75$. If $G = 0$, then a conventional least squares method is obtained (without weighting coefficients and without division by Φ_j in (42)). Unlike to parametric quadratic approximation commonly used in response surface method the minimization of approximating function is more difficult. Generally, any method of non-linear programming can be used. However, using the derivatives is not appropriate because the approximating function cannot be to smooth enough and may have a lot of local extremes. Two methods are employed in order to obtain a global minimum of locally approximated function of interest.

The first method is iterations. A randomly selected point in design space is a starting point. Then in this point the local approximation is performed and according (42) coefficients β are found. Then the minimum point of the approximating function is calculated with a fixed values of coefficients β. This is a simple problem, which needs to solve the system of five linear algebraic equations. Then in this new point a local approximation is built and the search is continued. One should be convinced that the true minimum is found. In the favorable case, when the process converges (and converges to the same point from the all starting points), there is high probability that the actual minimum was found. From the experience it can be concluded that in this case the physical parameters of plate are correctly identified. Unfortunately two alternative cases are found to be more common. In the first case the process can converge to the point outside of the region for which the experimental design was planned. Then a center of the experimental design (for FEM calculations) should be moved or the bounds should be shifted. The limits of the domain of interest can be shifted since there are no critical constraints for variables. In the worst case, when the iterative procedure diverges or gives a lot of local extremes, the second method is used - a direct search (Auzins et al. (1999)). About 100000 points from the randomly selected Latin hypercube type sample are tested and the best point is selected. Then the search domain is reduced around this point and new random search is performed while acceptable accuracy of extreme values is obtained. This is computationally more expensive way than iterative search, because one calculation of approximating function needs to solve the system of 21 linear equations (Cholesky decomposition method has been used). All process of minimization of functional (19) requires about one to two minutes of calculation time on a Pentium 800 MHz processor, but compared with the time of the FEM simulation this time is negligible. After the minimum of approximating function of interest is found, some confirmation N_a points near the optimum values should be calculated to verify the accuracy of identification. These points can be used as

additional points and optimization may be repeated employing $N + N_a$ design points to improve the accuracy of solution.

1.10 Results and Verification

Elastic constants for Cross-Play Plate. Let us consider the procedure of identification for the cross-ply glass/epoxy composite plates. A Latin hypercube (LHD) experiment design with four variables ($N = 4$) and 35 sample points ($K = 35$) was selected for the first set of variables Eq. (6). The LHD experiment design with five variables ($N = 5$) and 36 reference points ($K = 36$) was selected for the second set of variables Eq. (8).The upper and lower bounds (domain of interest) of the elastic constants for the first set of variables were taken as follows

$$\begin{aligned} 5 \text{ GPa} \leq\ & E_2 \leq 20 \text{ GPa}, \\ 3 \text{ GPa} \leq\ & G_{12} \leq 9 \text{ GPa}, \\ 3 \text{ GPa} \leq\ & G_{23} \leq 14 \text{ GPa}, \\ 0.2 \leq\ & \nu_{12} \leq 0.4 \end{aligned} \tag{43}$$

The upper and lower bounds of the elastic modulus E_1 for the second set of variables were selected by

$$33 \text{ GPa} \leq E_1 \leq 43 \text{ GPa}, \tag{44}$$

Constraints for other elastic constants were taken the same Eq. (43) as for the first set of variables.

For the first set of variables Eq. (6) the lower and upper bounds were recalculated by Eq. (3). For the second set of variables Eq. (8) the lower and upper bounds were recalculated by Eq. (2). By using the matrix B_{ij} of the experiment design ($N = 4$ and $K = 35$ for the first set of variables, $N = 5$ and $K = 36$ for the second set of variables) in the expression (27) the values of $\boldsymbol{x}$ were calculated for all reference points. Employing the values of parameter $\boldsymbol{x}$ in the reference points and the initial guess value $E_1^0 = 35$ GPa the first 20 natural frequencies in all K points were calculated. Similar calculations were performed also for the second set of variables $\boldsymbol{x}$.

The finite element mesh of the plate was shown in Fig. 5. It should be noted that there is some originality in calculation of the mass matrix $\boldsymbol{M}$ in equation (21). In order to represent more accurate an inertia forces of the plate, the mass of sensor m_s should be taken into account. In the finite element modelling it is assumed that the finite elements where the sensor is located (see Fig. 5) have the same thickness h as the plate, but for these finite elements an equivalent density ρ_{eqv} is calculated

$$\rho_{\text{eqv}} = \rho + \frac{m_{\text{s}}}{F_{\text{s}} h}$$

Here F_{s} is the area of the sensor.

The data of numerical simulations were used to build the response surfaces (39). For this the RESINT program (Eglais; Rikards (1981; 1993)) was employed. For the first set of variables approximating functions were obtained for frequencies. These functions were

used in the functional (10). For the second set of variables approximating functions were obtained for the eigenvalues. These functions were used in the functional (17).

For the second set of variables $\boldsymbol{x}$ as example two approximating functions (first and second eigenvalue) are given below

$$\begin{array}{lll} \lambda_1(\boldsymbol{x}) = 0.127 \cdot 10^7 & + 0.602 \cdot 10^6 z_5 & + 0.155 \cdot 10^5 z_2, \\ \lambda_2(\boldsymbol{x}) = 0.456 \cdot 10^7 & + 0.126 \cdot 10^7 z_2 & + 0.362 \cdot 10^6 z_1 \; - \\ \quad 0.304 \cdot 10^6 z_3 & + 0.240 \cdot 10^5 z_5 & - \\ \quad 0.133 \cdot 10^6 z_3^2 & + 0.443 \cdot 10^5 z_1 z_3 & \end{array} \tag{45}$$

Here normalized variables are introduced

$$\begin{aligned} z_1 &= -8.21 + 0.21 \cdot 10^{-9} A_{11}, \\ z_2 &= -1.61 + 0.12 \cdot 10^{-9} A_{22}, \\ z_3 &= -1.46 + 0.31 \cdot 10^{-9} A_{12}, \\ z_4 &= -1.55 + 0.18 \cdot 10^{-9} A_{44}, \\ z_5 &= -2.00 + 0.33 \cdot 10^{-9} A_{66} \end{aligned} \tag{46}$$

Correlation c of approximating functions with the FEM data for the first eigenvalue is $c = 0.979$ and for the second eigenvalue $c = 0.991$. Similar expressions were obtained for other eigenvalues. Note that transverse shear modulus is presented only in approximations for the higher eigenvalues, i.e., for the modes 9, 10 and 13. Influence of the transverse shear deformations on the first frequencies is small and therefore this variable is not presented in the all approximating functions.

The approximating functions were obtained using the step-by-step elimination procedure. The diagram of reduction of terms building the function for the second eigenvalue is shown in Fig. 15. It is seen that the first break in diagram corresponds to the regression equation with seven terms. At eliminating the seventh term the correlation with the data of numerical experiment decreases much more in comparison with the previous step. Eliminating further this term an accuracy of approximation can be lost. Thus, for the second eigenvalue the approximating function is selected with seven terms. It should be noted that polynomial terms were not selected *a priori*. These terms were obtained in the process of building the model and selected as the best regressors.

Depending on approximations in the identification different number of experimental eigenfrequencies were used. Thus, for the plate PU10 using the first set of variables in identification procedure the vector of weights (see Eq. (10)) is chosen as follows

$$\boldsymbol{w} = [0\ 1\ 0\ 1\ 1\ 1\ 1\ 1\ 1\ 1\ 1\ 1\ 1\ 1\ 0\ 0\ 0\ 0\ 1\ 0\ 0\ 0\ 0\ 0]$$

Note, that using in identification the first set of variables the first experimental frequency is taken into account indirectly, i. e., in the scaling (see Eq. (7)) but not directly in the functional Eq. (10). Thus, in this case at all 14 experimental frequencies are employed in identification.

For the same plate PU10 using the second set of variables in identification procedure the vector of weights (see Eq. (17)) was set different

$$\boldsymbol{w} = [1\ 1\ 0\ 1\ 1\ 0\ 0\ 0\ 0\ 1\ 1\ 0\ 0\ 1\ 0\ 0\ 0\ 0\ 0\ 0\ 0\ 0\ 0\ 0]$$

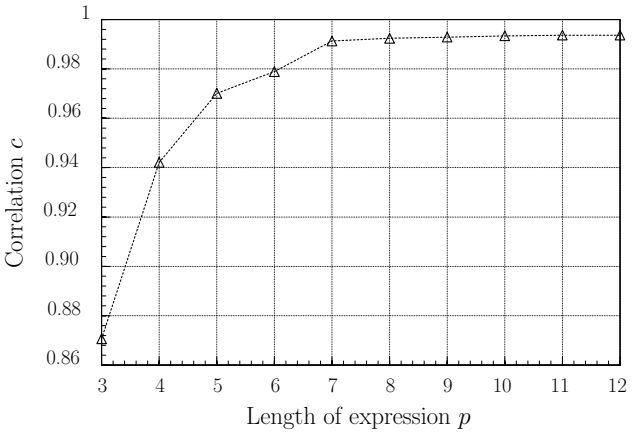

Figure 15. Diagram of term reduction for the function $\lambda_2(\boldsymbol{x})$

Thus, using for identification the second set of variables only seven experimental frequencies are employed. Such difference is due to different approximating functions. Here only the approximating functions with correlation $c > 0.90$ are employed.

For the plate PU11 using the first set of variables in identification procedure the vector of weights is as follows

$$\boldsymbol{w} = [0\ 1\ 0\ 1\ 1\ 1\ 0\ 1\ 1\ 1\ 1\ 0\ 1\ 1\ 0\ 0\ 0\ 0\ 1\ 0\ 0\ 0\ 0\ 0]$$

In this case at all 12 experimental frequencies are employed in identification. For the same plate PU11 using the second set of variables in identification procedure the vector of weights is given by

$$\boldsymbol{w} = [1\ 1\ 0\ 1\ 1\ 0\ 0\ 0\ 0\ 0\ 1\ 0\ 1\ 1\ 0\ 0\ 0\ 0\ 1\ 0\ 0\ 0\ 0\ 0]$$

In this case for identification only eight experimental frequencies are employed.

Minimization of the functional (10) or (17) subject to constrains was performed by the random search method (Rikards (1993)). For the second set of variables in addition a system of three non-linear equations (2) was solved. Results of identification of the layer stiffness properties for the two plates considered (PU10 and PU11) are presented in Table 6. Here in the columns noted by 1 and 2 the results obtained using in identification the first and second set of variables are presented.

It is seen that in-plane Young's moduli E_1 and E_2 and shear modulus G_{12} obtained by using different set of variables are in good agreement. Larger differences is for the Poisson's ratio ν_{12}. The reason is that influence of Poisson's ratio on frequencies is considerably smaller and in this case accuracy of approximation is not sufficient. The transverse shear modulus G_{23} is overestimated. The transverse shear modulus can not be reliable determined from the measured frequencies since the plates were too thin ($h/a = 1/70$) for identification of this property. In this case more thick plates should be used.

Table 6. Elastic properties of single layer.

	PU10		PU11	
Property	1	2	1	2
E_1, GPa	38.89	38.29	38.20	37.22
E_2, GPa	12.78	12.63	11.95	12.41
G_{12}, GPa	5.06	5.11	4.77	4.75
G_{23}, GPa	11.70	14.00	9.55	7.41
ν_{12}	0.304	0.350	0.392	0.426

Table 7. Flexural frequencies f_i (Hz) and residuals Δ_i for plates PU10 and PU11.

	PU10			PU11		
Mode i	Exp.	FEM	Δ_i (%)	Exp.	FEM	Δ_i (%)
1	166	166.4	+0.24	159	158.5	-0.31
2	341	344.2	+0.94	332	332.1	+0.03
3	–	416.2	–	–	407.3	–
4	484	486.1	+0.43	464	470.1	+1.31
5	542	545.9	+0.72	529	526.9	-0.40
6	902	895.6	-0.71	869	866.8	-0.25
7	971	967.5	-0.36	938	944.0	+0.64
8	1090	1087	-0.28	1050	1050	0
9	1155	1165	+0.87	1143	1134	-0.79
10	1273	1278	+0.39	1240	1247	+0.56
11	1523	1513	-0.66	1470	1469	-0.07
12	1643	1632	-0.67	–	1584	–
13	1898	1865	-1.74	1838	1814	-1.30
14	2003	2001	-0.10	1940	1950	+0.51
15	2290	2218	-3.14	2180	2155	-1.15
16	–	2275	–	2212	–	
17	2418	2379	-1.61	2338	2314	-1.03
18	–	2414	–	–	2355	–
19	2733	2724	-0.33	2665	2657	-0.30
20	–	3010	–	–	2923	–
21	3108	3157	+1.58	3023	3074	+1.69
22	3223	3226	+0.22	3135	3141	+0.19
23	–	3315	–	–	3230	–
24	3605	3617	+0.33	–	3522	–

Verification of the results was performed by the finite element method (FEM) and through the independent experiments. For the finite element analysis the elastic constants

obtained by the identification procedure were used (see Table 6). Results are shown in Table 7. Residuals were calculated by the expression

$$\Delta_i = \frac{f_i^{\mathrm{FEM}}(\boldsymbol{x}^*) - f_i^{\mathrm{exp}}}{f_i^{\mathrm{exp}}} \times 100 \tag{47}$$

It is seen that differences between the experimental and numerical frequencies calculated by using elastic constants obtained by identification are very small. Mostly residuals do not exceed 1%. Exception is for the mode 15 of the plate PU10 since in this case the difference is 3.14%. Note that for the verification at all 19 (plate PU10) and 17 (PU11) experimental frequencies are used but for the identification considerably smaller number of frequencies were taken into account. Predicted frequencies (see Table 7) which were not taken into account for identification also are in good agreement with the experimental ones.

It is of interest to compare the elastic constants of the single layer of the cross-ply glass/epoxy laminate with the properties obtained for the unidirectionally (UD) reinforced transversely isotropic plate made from the same material (Bledzki et al. (1999)). Results are presented in Table 8. For the cross-ply laminate the mean values calculated from four values of Table 6 are shown. Good agreement of the results for the constants E_1, E_2 and G_{12} is observed. However, there is some difference for the Poisson's ratio. It can be explained since this property is less sensitive to frequencies as modulus of elasticity, especially for the cross-ply laminate. Due to approximations an accuracy for the Poisson's ratio has been lost. Soares et al. (1993) has shown that good accuracy for the Poisson's ratio can be obtained employing in minimization the original (numerical) functions instead of approximating functions. Below on example of identification of elastic properties for carbon/epoxy plates it will be shown that using local approximations the accuracy can be increased and also the Poisson's ratio can be determined accurately.

Table 8. Comparison of results for cross-ply and unidirectional laminates.

Property	Cross-ply plate	UD plate
E_1, GPa	38.15	38.81
E_2, GPa	12.44	12.12
G_{12}, GPa	4.92	5.09
ν_{12}	0.368	0.255

Elastic constants for carbon/epoxy laminate For this material response surfaces were built employing local approximations. To build the local approximations the experimental MMSDLH type design with $N = 101$ sample points in five dimensions are used. These sample points are distributed in the domain of interest, which is formed by lower and upper limits of variables

$$x_i^{\min} \le x_i \le x_i^{\max} \tag{48}$$

The upper and lower limits for variables are selected employing the initial guess values of elastic constants. These values can be taken from the properties of similar material or from the static test of the present material. In the process of search the limits can be moved, if, for example, the identified constants are beyond the limits, or if the accuracy of search should be increased. In a sample points ($j = 1, 2, , N$) the equation (21) was solved and eigenvalues $\lambda_i(x_j)$ were obtained. These eigenvalues are treated as functions forming the original function through expressions (17) or (19). Approximations $\hat{\Phi}(x)$ of the original function (17) or (19) were obtained using the local approximation method described above. In the functional (19) mainly the power $m = 1$ was used.

Experimentally measured frequencies, which are presented in Table 4, can be used in identification in any combination. A cross validation for all sample points was performed in order to achieve better approximation of the original function and to select the most important (most sensitive to elastic constants) and reliable frequencies. In order to improve the process of identification a user's friendly software with a dialog has been developed. Results of identification for all seven plates are presented in Table 9. The average values and standard deviations are calculated. Analyzing the values in the last column (standard deviations in percents) it is seen that elastic modulus in the fiber direction E_1, the transverse modulus E_2, the in-plane shear modulus G_{12} and the Poisson's ratio ν_{12} can be determined with a sufficient confidence. In the same time the transverse shear modulus G_{23} cannot be statistically confident determined since the standard deviation is too large. The reason is that there is small influence of this modulus to frequencies. The sensitivity of this parameter is comparable with a systematic and statistical errors of the experiment.

Table 9. Identified elastic constants of CFRP laminate

	UD1	UD2	UD3	UD4	UD5	UD6	UD7	Average σ	$\sigma, \%$
E_1	171.69	165.30	172.46	159.75	170.69	159.37	159.73	165.57	6.022	3.64
E_2	10.40	10.05	10.95	11.08	11.21	11.194	9.282	10.672	0.400	3.75
G_{12}	6.14	5.97	6.36	6.14	6.35	6.312	5.690	6.137	0.255	4.16
G_{23}	8.73	10.60	5.32	11.94	9.98	9.096	8.983	9.235	2.061	22.3
ν_{12}	0.328	0.329	0.339	0.347	0.329	0.357	0.322	0.3359	0.011	3.28

It is of interest to evaluate the accuracy of identification. Verification of the results was performed calculating by FEM the original function in the point of optimum. In Table 10 evaluation for the plate UD1 is given. The frequencies marked with a sign (*) were used in identification. For this plate the best accuracy was obtained employing the following combination of frequencies f_i ($i = 1, 2, 3, 4, 6, 7, 8, 13$). Thus for this plate at all 8 frequencies were used for identification of 5 constants. The numerical values obtained by FEM in the point of optimum have been compared with the experimental frequencies.

Residuals Δ_i^1 characterizing the differences between experimental and numerical (FEM) frequencies were calculated by the expression

$$\Delta_i^1 = \frac{f_i^{\exp} - f_i^{FEM}(x*)}{f_i^{\exp}} 100 \tag{49}$$

It is seen that differences between experimental and numerical frequencies are very small. The residuals do not exceed 1%, even for those frequencies, which were not used in identification (frequencies i=5,15,16,17). However, since in general higher frequencies are less sensitive to elastic constants that lower frequencies, in addition to residuals Δ_i^1 the range of each frequency in the experiment design space should be compared. In the last column of Table 10 the relative amplitude of frequencies Δf_i in the experiment design space is presented. The relative amplitude is calculated by the expression

$$\Delta f_i = \frac{f_i^{\max} - f_i^{\min}}{f_i^{\exp}} 100 \tag{50}$$

Here

$$f_i^{\max} = \max_{x^j} f_i(x^j), \quad f_i^{\min} = \min_{x^j} f_i(x^j) \tag{51}$$

In Table 10 it is seen that lower frequencies are more sensitive to the elastic constants. However, the amplitude in the design space for the $8th$ and $13th$ frequency is also considerable.

Table 10. Calculation of residuals for plate UD1

No.	f_i^{FEM}, Hz	f_i^{exp}, Hz	Δ_i^1, %	Δf_i, %
1*	97.7	97	-0.72	11.15
2*	124.0	123.8	-0.16	6.94
3*	235.2	237.4	+0.93	9.39
4*	341.6	341	-0.18	6.89
5	454.6	458	+0.74	8.12
6*	503.5	502.6	-0.18	1.43
7*	540.5	541.2	+0.13	2.69
8*	651.7	653	+0.20	5.07
9	675.5	–	–	–
10	779.1	–	–	–
11	861.4	–	–	–
12	1112	–	–	–
13*	1170	1168	-0.17	7.96
14	1215	–	–	–
15	1380	1381	+0.07	1.52
16	1411	1413	+0.14	2.05
17	1507	1512	+0.33	3.04

It is of interest to explain how the frequencies used in identification were selected. Note that in identification the functionals (17) or (19) were employed. In the first case each frequency (eigenvalue) was approximated, but in the second case the approximation was performed for the functional (19). For illustration in Table 11 selection of frequencies for the plate UD7 is presented. Performing approximations for each frequency the value of approximating function f_i^{appr} is calculated and frequencies with smaller approximation error were selected. Preference is given for the lowest frequencies. Selected frequencies are marked with the (*) sign. In the point of optimum x* two additional residuals Δ_i^2 and Δ_i^3 were calculated

$$\Delta_i^2 = \frac{f_i^{\exp} - f_i^{FEM}(x*)}{f_i^{FEM}(x*)} 100 \tag{52}$$

$$\Delta_i^3 = \frac{f_i^{appr}(x*) - f_i^{FEM}(x*)}{f_i^{FEM}(x*)} 100 \tag{53}$$

Residuals Δ_i^2 are used in the selection of frequencies for identification. Preference is given for the lowest frequencies with smaller residuals Δ_i^2 . Note that residual Δ_i^3 characterizes a difference between the original function obtained by FEM and approximating function obtained by using experiment design and local approximations (41). It is seen that local approximations are very accurate.

Table 11. Selection of frequencies for plate UD7.

No.	$f_i^{\exp}$	$f_i^{appr}(x*)$	$f_i^{FEM}(x*)$	Δ_i^2, %	Δ_i^3, %
1	299.0*	299.06	299.1	-0.033	-0.013
2	377.5*	380.05	380.0	-0.658	0.013
3	720.5*	714.46	714.5	0.840	-0.006
4	1046*	1041.90	1042	0.384	-0.009
5	1388	1372.37	1372	1.166	0.027
6	1512*	1517.38	1517	-0.340	0.025
7	1630.5*	1626.36	1626	0.277	0.022
8	1959*	1954.09	1954	0.256	0.005
9	–	–	2041	–	–
10	–	–	2337	–	–
11	2569	2553.81	2554	0.587	0.007
12	3370	3335.06	3335	1.049	0.002
13	–	–	3436	–	–
14	–	–	3612	–	–
15	4032.5	4003.14	4003	0.737	0.003
16	4141	4089.04	4089	1.271	0.001
17	4386	4350.98	4351	0.804	-0.000
18	–	–	4628	–	–

Similarly residuals Δ_i^1 , Δ_i^2 and Δ_i^3 were calculated for all seven plates. Frequencies obtained by the finite element solution (original function) with the identified elastic constants (Table 9) for four plates are presented in Table 12. With the sign (*) are marked the experimental frequencies used in identification. It is seen that even for the frequencies, which were not used in identification, there is good agreement between numerical (FEM) and experimental frequencies.

Table 12. Experimental (f_i^{exp}) and FEM (f_i^{FEM}) frequencies [Hz] and modes.

No.	m, n	UD1		UD2		UD3		UD4	
		f_i^{exp}	f_i^{FEM}	f_i^{exp}	f_i^{FEM}	f_i^{exp}	f_i^{FEM}	f_i^{exp}	f_i^{FEM}
1	1, 1	97.0*	97.7	97.6*	97.8	98.2*	98.2	97.5*	97.7
2	2, 0	123.8*	124.0	123.4*	123.8	126.0*	125.7	125.0*	124.9
3	2, 1	237.4*	235.2	245.0	235.4	237.0*	237.0	236.0*	235.9
4	3, 0	341.0*	341.6	342.0*	341.1	345.6*	346.3	344.0*	344.2
5	3, 1	458.0	454.6	–	454.7	457.0	458.8	457.5	457.2
6	0, 2	502.6*	503.5	501.0*	501.8	498.0*	499.1	497.0*	497.8
7	1, 2	541.2*	540.5	538.0*	539.0	536.5*	536.8	537.5	535.5
8	2, 2	653.0*	651.7	653.0*	650.9	654.0	650.8	650.0*	649.0
9	4, 0	–	675.5	–	674.6	–	683.3	682.5	680.7
10	4, 1	–	779.1	–	779.1	780.0	786.9	784.0	784.9
11	3, 2	–	861.4	866.0*	861.2	863.0*	861.9	866.0	861.4
12	5, 0	–	1112	1124.5	1111	1125*	1126	1124.5	1122
13	4, 2	1168*	1170	–	1171	–	1174	–	1175
14	5, 1	–	1215	–	1215	1242	1227	–	1225
15	0, 3	1381	1380	–	1375	1368.5*	1368	1365.5	1364
16	1, 3	1413	1411	–	1406	1401.6*	1400	1402.5	1397
17	2, 3	1512	1507	–	1503	1506.5	1497	1504	1494
18	5, 2	–	1592	1589*	1594	–	1599	–	1604

In order to validate results obtained from the vibration tests through identification it is necessary to compare elastic properties of the present carbon/epoxy laminate obtained from an independent test. Conventional static test was selected as independent test. Static tests were performed according to ASTM guidelines (results of RTU - Riga Technical University and IAI - Israel Aircraft Industry) and DIN standards (results of DLR - German Aerospace Center). Test results are presented in Table 13. In parentheses the values obtained by the static compression test are given. In general good agreement of the results is observed. However, it is open whether the transverse shear modulus G_{23} could be reliably determined from the present vibration test.

Elastic constants of the composite laminates can be reliable determined employing the identification procedure based on the experiment design and response surface method. For this Latin Hypercube (LHD) and minimal Mean Squared Distance (MSD) designs are employed. Global polynomial as well as and local approximations can be used to built

Table 13. Comparison of elastic constants obtained from vibration and static tests.

Elastic constant	Vibration test	Static test		
		RTU	IAI	DLR
E_1, GPa	165.6	176 (143)	165 (175)	192 (147)
E_2, GPa	10.67	8.9 (9.6)	9.2 (11.8)	10.6 (9.7)
G_{12}, GPa	6.14	5.2	5.4	6.1
G_{23}, GPa	9.23	–	–	–
ν_{12}	0.336	0.34	–	0.31 (0.34)
ν_{12}	0.336	0.34	–	0.31 (0.34)

the response surfaces. It was shown that the in-plane elastic constants obtained from vibration tests through identification are in good agreement with the values obtained by conventional static tests.

1.11 Damage identification in laminates

Today there are strong needs and requirements for on-line damage (delamination) detection and health monitoring techniques on composite structures. Currently available non-destructive evaluation (NDE) methods are mostly non-model methods, i.e., either visual or localized experimental methods, such as acoustic or ultrasonic methods, magnetic field methods, radiographs, eddy-current methods and thermal field methods (see, e.g., Doebling et al. (1996)). Accessing these methods are time consuming and costly. Almost all of these techniques require that the vicinity of the damage is known in advance. Subject to these limitations, these non-model (experimental) methods can provide only local information and no indication of a structural strength at a system level.

Shortcomings of currently available NDE methods indicate a requirements of damage inspection techniques that can give global information on the structure. This requirement can led to the development of model-based numerical-experimental methods that examine changes in vibration characteristics of the composite structure.

The model-based (MB) methods undertake analysis of structural models and are usually implemented by finite element analysis. Damage or delaminations is simulated by modifying the models. Experimental data then be compared with the analytical data to determine damage location and extent. The effectiveness of the MB techniques, however, is dependent on the accuracy of the structural model and these methods may have difficulties when applied to complex structures due to uncertainties in boundary conditions, loading conditions, etc. The model-based methodologies can be classified in the following categories (Zou et al. (2000)).

1. Modal analysis methods.
2. Frequency domain methods.
3. Time domain methods.
4. Impedance domain methods.

Modal analysis methods. This group of methods utilize the information from all modal parameters (modal frequencies, mode shapes and modal damping ratio) or combinations of some of them to detect damage. The basic idea of these methods is that modal parameters are functions of physical properties of the structure (mass, stiffness and damping). Therefore, changes in physical properties due to damage will cause changes in the modal properties. Usually, damage will decrease mass and stiffness and increase damping ratio locally. Among the three structural properties, mass is less sensitive to damage while damping is most sensitive to damage.

According to their different detection techniques, the modal analysis methods can be divided into the following major categories (Zou et al. (2000)).

- Modal shape changes methods.
- Modal shape curvature methods.
- Sensitivity based update methods.
- Eigenstructure assignment methods.
- Optimal matrix update methods.
- Changes in measured stiffness matrix methods.
- Frequency response function methods.
- Combined modal parameters methods.

The majority of this group of methods uses the lower frequencies and can best describe the global behavior of structure, however, e.g, the mode shape curvature methods are promising in detection of localization of damage. Major advantage of these methods is that the modal information is cheap to obtain and easy to extract.

Frequency domain methods. Damage may be detected using frequency response of the structure. The damage produces a decrease in structural stiffness, which, in turn, produces decreases in natural frequencies (see, e.g., Satawu (1997)). The current frequency domain methods are either using lower frequencies for providing global information or using higher frequencies for providing local information of structures. None of these can provide sufficient information for the detection of both small and large defects.

Time domain methods. Basically, all methods in this category are related because they use time history. These methods could be independent of modal information although they are usually combined with frequency domain methods. Damage is estimated using time history and vibration responses of the structure.

Impedance domain methods. Damage is detected through measuring the changes of impedance in the structure. The basis of this technique is that each part of the structure contributes to the impedance of structure to some extent. Any variation in the structure integrity will generally result in changes in the impedance, i.e., impedance will change with changes of the stiffness. Impedance domain methods are particularly suitable for detecting planar defects such as delaminations.

In general vibration model-based methods combined with modal analysis provide global as well as local information on structural health condition and do not require

direct human accessibility to the structure. The methods are cost effective and easy to operate, and has a potential for on-line damage detection with appropriate structural modelling. However, there are large differences in laboratory experiments and response of the real structures. Laboratory experiments are often conducted under tightly controlled repeatable conditions to ensure that the changes are only due to the self-created damage. Therefore, to develop practical and capable on-line damage detection method of real structures a large amount of research should be performed.

Example of damage identification. Let us consider a glass-epoxy cross ply laminated plate loaded with impact loading. After impact loading the plate is damaged. There is damage and delamination area which should be identified in order to evaluate the load carrying capacity of the damaged structure. Elastic constants of these plates before damage were identified in section 1.10. Geometric dimensions of the plate PE08 are as follows

$$a = 140.3 \text{ mm},\ b = 139.9 \text{ mm},\ h = 2.067 \text{ mm},\ \rho = 140.3 \text{ kg/mm}^3$$

In identification of elastic properties of this cross-ply plate having eight layers with the layer stacking sequence $[90/0/90/0]_s$ at all 17 frequencies were taken into account. For simplicity the laminated plate is assumed as orthotropic plate with homogeneous properties in the thickness direction. Note that in section 1.10 the cross-ply plate was assumed be with the discrete layers and elastic properties were identified for a single layer. Here the homogeneous orthotropic properties are identified. The values obtained are as follows

$$E_x = 21.15 \text{ GPa},\ E_y = 29.83 \text{ GPa}, G_{xy} = 5.24 \text{ GPa},$$

$$G_{xz} = G_{yz} = 4.11 \text{ GPa},\ \nu_{xy} = 0.191$$

Elastic modulus E_y of the undamaged plate is higher since the fiber direction of the outer layers is in y direction (see Fig. 1).

Further the plate is loaded by 5 and 10 repeated impact loadings. The damaged plate after 5 impacts is shown in Fig. 16. It is seen the damage and delaminations in the impact zone. Again experimental frequencies of the damaged plate are measured. The frequencies of undamaged and damaged plate (after 5 and 10 impacts) are presented in Fig. 17. It is seen that for the damaged plate reduction of frequencies is about one to five percents.

The damaged area is clearly seen in the center of the glass/epoxy plate. It is assumed that the shape of damaged area is a square with dimensions 63.6×63.6 mm^2. In the damaged area the stiffness is reduced and elastic constants is lower. The scalar damage parameters d_i can be introduced in order to take into account the reduction of stiffness

$$E_x^* = d_1 E_x,\ E_y^* = d_2 E_y, G_{xy}^* = d_3 G_{xy} \tag{54}$$

The identification of damage parameters d_i is similar as identification of elastic constants. For the plate after 5 impacts the following values have been identified

$$d_1 = d_2 = 0.65,\ d_3 = 0.43,\ E_x^* = 13.80 \text{ GPa},\ E_y^* = 19.63 \text{ GPa},\ G_{xy}^* = 2.26 \text{ GPa}$$

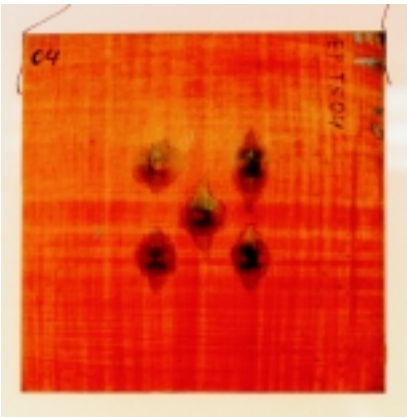

Figure 16. Damaged cross-ply laminated glass/epoxy plate after 5 impacts.

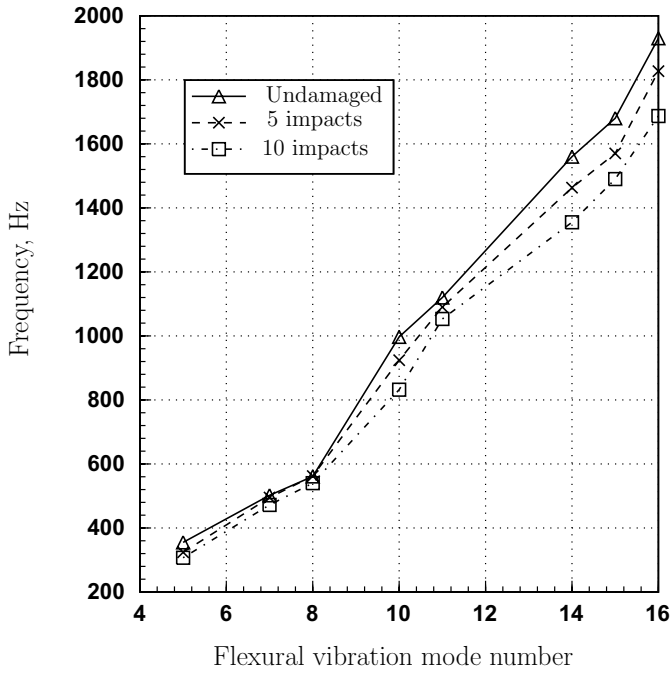

Figure 17. Frequency reduction of damaged glass-epoxy cross-ply plate.

However, it should be noted that more accurate damage identification can be performed taking into account also the mode shapes (mode curvatures), not only the frequencies.

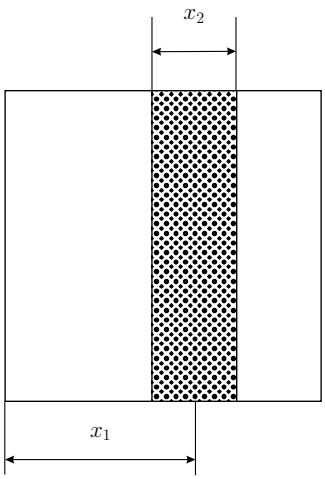

Figure 18. Location of damage zone of plate.

In the example discussed above the shape, localization and dimensions of the damaged zone was detected by optical inspection. In many cases such inspection is impossible to perform. Then the shape, localization and dimensions of the damaged zone should be identified employing the same numerical-experimental (model-based) methodology used above.

Let us consider a numerical experiment in order to identify the size and location of a damage zone of the composite plate (see Fig. 18). In this case there are two parameters of identification: the location of the center of the damage zone x_1 and the width of the damage zone x_2. The damage of the transversely isotropic plate is introduced by reducing the stiffness of the damaged zone

$$E_1^* = x_3 E_1,\ E_2^* = x_3 E_2, G_{12}^* = x_3 G_{12} \tag{55}$$

In the numerical experiment it was assumed that $x_3 = 0.5$ and the location of the damaged zone in the rectangular orthotropic plate ($a = b = 0.140$ m, h=2 mm) is given by $x_1^{\exp} = 0.591a$ and $x_2^{\exp} = 0.273a$. The finite element mesh was taken 22×22, i. e., the same as for the examples considered above (see Fig. 5). Employing these parameters the finite element model of the damaged plate was created. Further the 10 lowest eigenfrequencies of the damaged plate were calculated by solving the eigenvalue problem (21). These numerical frequencies were assumed as experimental frequencies of the damaged plate. Then the Latin hypercube experiment design with 25 sample points was used. The domain of interest was assumed as follows

$$0.5a \le x_1 \le 0.7a,\ 0.15a \le x_2 \le 0.35a$$

In this domain of interest location of 25 reference points was calculated by Eq. (27). In these sample points the 10 first eigenfrequencies were calculated by the finite element

method. Employing these data the approximating functions were obtained for all 10 frequencies. These functions were used in the identification functional (10). Minimizing this functional the folowing parameters were obtained

$$x_1^* = 0.589a,\ x_2^* = 0.274a$$

It is seen that through the identification procedure about the same values of location and size of the damaged zone, which were introduced in the numerical experiment, have been obtained. It should be noted that for both examples - identification of elastic constants and location of the damage zone - the uniqueness of solution can be proved. Acctually, in both cases the stiffness matrix $\boldsymbol{K}$ of the eigenvalue problem (21) is a linear function of the parameters of identification x. In this case the eigenvalues (natural frequencies) are convex functions of x. This statement was proved by Rikards et al. (2001). Therefore, the functional (10) to be minimized is convex and the solution of identification examples discussed here is unique.

References

Altenbach, H., Altenbach, J., Rikards, R. (1996). Einfürung in die Mechanik der Laminat- und Sandwichtragwerke: Modellierung und Berechnung von Balken und Platten aus Verbundwerkstoffen. Stuttgart: Deutscher Verlag für Grundstoffindustrie.

Audze, P. and Eglais, V. (1977). New approach to planning out of experiments. In: *Problems of Dynamics and Strength. Vol.35*, E. Lavendel, ed., Zinatne, Riga, pp. 104-107 (in Russian).

Auzins, J., Janushevskis, A. and Onzevs, O. (1999). Optimization of Multibody Vibration Response by Global Search Procedure,. In: *Proceedings of ECCM 99, European Conference on Computational Mechanics*, CD-ROM, Munich, Germany, p. 17.

Auzins, J and Janushevskis, A. (2002). New Experimental Designs for Metamodelling and Optimization. In: *Proceedings of WCCM V, Fifth World Congress on Computational Mechanics, July 7 - 12, 2002,Vienna, Austria*, CD-ROM edition, pp. 1-10.

Barthelemy, J.-F. M. and Haftka, R. T. (1993). Approximation concepts for optimum structural design - review. *Structural Optimization* 5:129–144.

Bathe, K.-J. (1982). *Finite Element Procedures in Engineering Analysis*, Englewood Cliffs:Prentice-Hall.

Bledzki, A. K., Kessler, A., Rikards, R. and Chate A. (1999). Determination of elastic constants of glass/epoxy unidirectional laminates by the vibration testing of plates. *Composites Science & Technology* 59:2015-2024.

Bolognini, L., Riccio, F., and Bettianli, F. (1993). A modal technique for the identification of stiffness and mass parameters in large structures. In: *Computational Methods and Experimental Measurements VI, Vol. 2: Stress Analysis*, C.A. Brebbia and G.M. Carlomagno, eds., Elsevier Applied Science, London-New York, pp. 337–352.

Box, G. E. P. and Draper, N. R. (1987). *Empirical Model-Building and Response Surfaces*, New York:Wiley.

Chakraborty, S. and Mukhopadhyay, M. (2000). Estimation of In-Plane Elastic Parameters and Stiffener Geometry of Stiffened Plates. *J. Sound and Vibration* 231(1): 99–124.

Cleveland, W. S. and Devlin, S. J. (2000). Locally Weighted Regression: An Approach to Regression Analysis by Local Fitting. *Journal of the American Statistical Association* 83:596–610.

Currin, C., Mitchell, T., Morris, D. and Ylvisaker, D. (1991). Bayesian Prediction of Deterministic Functions with Applications to the Design and Analysis of Computer Experiments. *Journal of the American Statistical Association* 86:953–963.

De Visscher, J., Sol, H., De Wilde, W. P., and Vantomme J. (1997). Identification of damping properties of orthotropic composite materials using a mixed numerical experimental method. *Appl. Compos. Mater.* 4(1): 13–33.

Doebling, S. W., Farrar, Ch. R., Prime, M. B. and Shevitz, D. W. (1996). Damage identification and health monitoring of structural and mechanical systems from changes in their vibration characteristics: A literature review. *Report LA-13070-MS, Los Alamos National Laboratory, New Mexico.*

Dyn, N., Levin, D. and Rippa, S. (1986). Numerical Procedures for Surface Fitting of Scattered Data by Radial Basis Functions. *SIAM Journal of Scientific and Statistical Computing* 7(2):639–659.

Eglais, V. (1981). Approximation of data by multi-dimensional equation of regression. In: *Problems of Dynamics and Strength. Vol. 39*, E. Lavendel ed., Zinatne, Riga, pp. 120–125 (in Russian).

Fang, K.-T. and Wang, Y. (1994). *Number-Theoretic Methods in Statistics*. London:Chapman & Hall.

Fang, K. T., Shiu, W.C. and Pan, J.X. (1999). Uniform Designs Based on Latin Squares *Statistica Sinica* 9:905–912. <www http://www.math.hkbu.edu.hk/UniformDesign/>

Frederiksen, P. S. (1997a). Experimental procedure and results for the identification of elastic constants of thick orthotropic plates. *J. Compos. Mater.* 31(4): 360–382.

Frederiksen, P. S. (1997b). Application of an improved model for the identification of material parameters. *Mech. Compos. Mater. and Struct.* 4:297–316.

Frederiksen, P. S. (1997c). Numerical studies for the identification of elastic constants of thick orthotropic laminates. *Eur. J. Mech. A/Solids* 16:117–140.

Frederiksen, P. S. (1998). Parameter unsertainty and design of optimal experiments for the estimation of elastic constants. *Int. J. Solids structures* 35: 1241–1260.

Friedman, J. H. (1998). Multivariate Adaptive Regression Splines. *The Annals of Statistics* 19(1):1–67.

Giunta, A. A., Dudley, J. M., Narducci, R., Grossman, B., Haftka, R. T., Mason, W. H. and Watson, L. T. (1994). Noisy Aerodynamic Response and Smooth Approximations in HSCT Design. In: *Proceedings of the 5th AIAA/USAF/NASA/ISSMO Symposium on Multidisciplinary Analysis and Optimization, Panama City Beach, FL, Sept. 1994*, pp.1117-1128.

Grediac, M. and Vautrin, A. (1993). Mechanical characterization of anisotropic plates: experiments and results. *Eur. J. Mech. A/Solids* 12(6): 819–838.

Haftka, R. T., Scott, E. P. and Cruz, J. R. (1998). Optimization and experiments: A survey. *Appl. Mech. Rev.* 51(7):435–448.

Hardy, R. L. (1971). Multiquadratic Equations of Topography and Other Irregular Surfaces. *J. Geophys. Res.* 76:1905–1915.

Johnson, M. E., Moore, L. M. and Ylvisaker, D. (1990). Minimax and Maximin Distance Designs. *Journal of Statistical Planning and Inference* 26(2):131–148.

Jones, R. M. (1975). Mechanics of Composite Materials. Tokyo: McGraw-Hill.

Khuri A. I. and Cornell J. A. (1996). Response Surfaces: Designs and Analyses. New York: Marcel Dekker.

Knauss, W. (2000). Perspectives in experimental mechanics. *Int. J. Solids Structures* 37: 251–266.

Koehler, J. R. and Owen, A. B. (1996). Computer Experiments. In: *Handbook of Statistics*, Ghosh, S. and Rao, C. R., eds., Elsevier Science, New York, 1996, pp. 261–308.

McKay, M. D., Conover, W. J. and Beckman, R. J. (1979). A comparison of Three Methods for Selecting Values of Input Variables in the Analysis of Output from a Computer Code. *Technometrics* 21(2):239–245.

Meyer, R. D., Steinberg D. M. and Box, G. (1995). Follow-Up Designs to Resolve Confounding in Multifactor Experiments. *Technometrics* 38:303–313.

Morris, M. D. and Mitchell, T.J. (1995). Exploratory designs for computer experiments. *Journal of Statistical Planning and Inference* 43:381-402.

Palmer, K. and Tsui, K.-L. (2001). A Minimum Bias Latin Hypercube Design. *IIE Transactions* 33(9):793-816.

Park, J.-S. (1994). Optimal Latin-Hypercube Designs for Computer Experiments. *Journal of Statistical Planning and Inference* 39(1):95–111.

Pedersen, P. (1989). Optimization method applied to identification of material parameters. In: *Discretization Methods and Structural Optimization - Procedures and applications*, H. A. Eschenauer and G. Thierauf, eds., Springer Verlag, Berlin, pp. 277–283.

Powell, M. J. D. (1987). Radial Basis Functions for Multivariable Interpolation: A Review,. In: *Algorithms for Approximation*, Mason, J. C. and Cox, M. G., eds., Oxford University Press, London, 1987, pp. 143–167.

Reddy, J. N. (1996). *Mechanics of Laminated Composite Plates. Theory and Analysis*. Boca Raton: CRC Press.

Rikards, R., (1993). Elaboration of optimal design models for objects from data of experiments. In: *Optimal Design with Advanced Materials. Proceedings of the IUTAM Symposium, Lyngby, Denmark, 18 - 20 August, 1992*, P. Pedersen, ed., Elsevier Science Publishers, Amsterdam, pp. 148–162.

Rikards, R. and Chate, A. (1995). Optimal design of sandwich and laminated composite plates based on planning of experiments. *Structural Optimization* 10 (1): 46–53.

Rikards, R. and Chate, A. K. (1997). Vibration and Damping Analysis of Laminated Composite and Sandwich Shells. *Mechanics of Composite Materials and Structures* 4:209–232.

Rikards, R., Chate, A., Steinchen, W., Kessler, A., and Bledzki, A. K. (1999). Method for identification of elastic properties of laminates based on experiment design. *Composites. Part B* 30:279-289.

Rikards, R., Chate, A. K. and Gailis, G. (2001). Identification of Elastic Properties of Laminates Based on xperiment Design. *Int. Journal of Solids and Structures* 38:5097–5115.

Roux, W. J., Stander, N. and Haftka, R. T. (1998). Response surface approximations for structural optimization. *Int. J. Numer. Meth. Engng.* 42: 517–534.

Sacks, J., Schiller, S. B. and Welch, W. J. (1989a). Design of Computer Experiments. *Technometrics* 31:41–47.

Sacks, J., Welch, W. J., Mitchell, T. J. and Wynn, H. P. (1989b). Design and Analysis of Computer Experiments. *Statistical Science* 4(4):409–435.

Salawu, O. S. (1997). Detection of structural damage through changes in frequency:A review. *Engineering Structures* 19:718–723.

Shewry, M. and Wynn, H. (1987). Maximum Entropy Design. *Journal of Applied Statistics* 14(2):165-170.

Soares, M. C. M., Moreira de Freitas, M., and Araújo A. L. (1993). Identification of material properties of composite plate specimens. *Composite Structures* 25: 277–285.

Sol, H., De Visscher, J., and De Wilde, W. P. (1993). Identification of the viscoelastic material properties of orthotropic plates using a mixed numerical/experimental technique. In: *Computational Methods and Experimental Measurements VI, Vol. 2: Stress Analysis*, C.A. Brebbia and G.M. Carlomagno, eds., Elsevier Applied Science, London-New York, pp. 131–142.

Tang, B. (1993). Orthogonal Array-Based Latin Hypercubes. *Journal of the American Statistical Association* 88(424):1392–1397.

Toropov, V. V. (1989). Simulation approach to structural optimization. *Structural Optimization* 1:37–46.

Toropov, V.V., Alvarez, L.F. (1998). Application of genetic programming and response surface methodology to optimization and inverse problems. In: *Inverse Problems in Engineering Mechanics. Proc. Int. Symposium, Nagano City, Japan, March 24-27, 1998*, M. Tanaka, G.S. and Dulikravich, eds., Elsevier, pp. 551–560.

Ye, K. Q. (1998). Column Orthogonal Latin Hypercubes and their Application in Computer Experiments. *Journal of American Statistical Association* 93:1430–1439.

Zou, Y., Tong, L. and Steven, G. P. (2000). Vibration based model dependent damage (delamination) identification and health monitoring for composite structures - a review. *J. Sound and Vibration* 230 (2):357–378.